The Danish Meteorological Institute

Ice and metocean conditions in and off Kong Oscar Fjord, East Greenland

Report for COWI

DMI Report 21-43
28 January 2022

Mads Hvid Ribergaard and Jørgen Buus-Hinkler

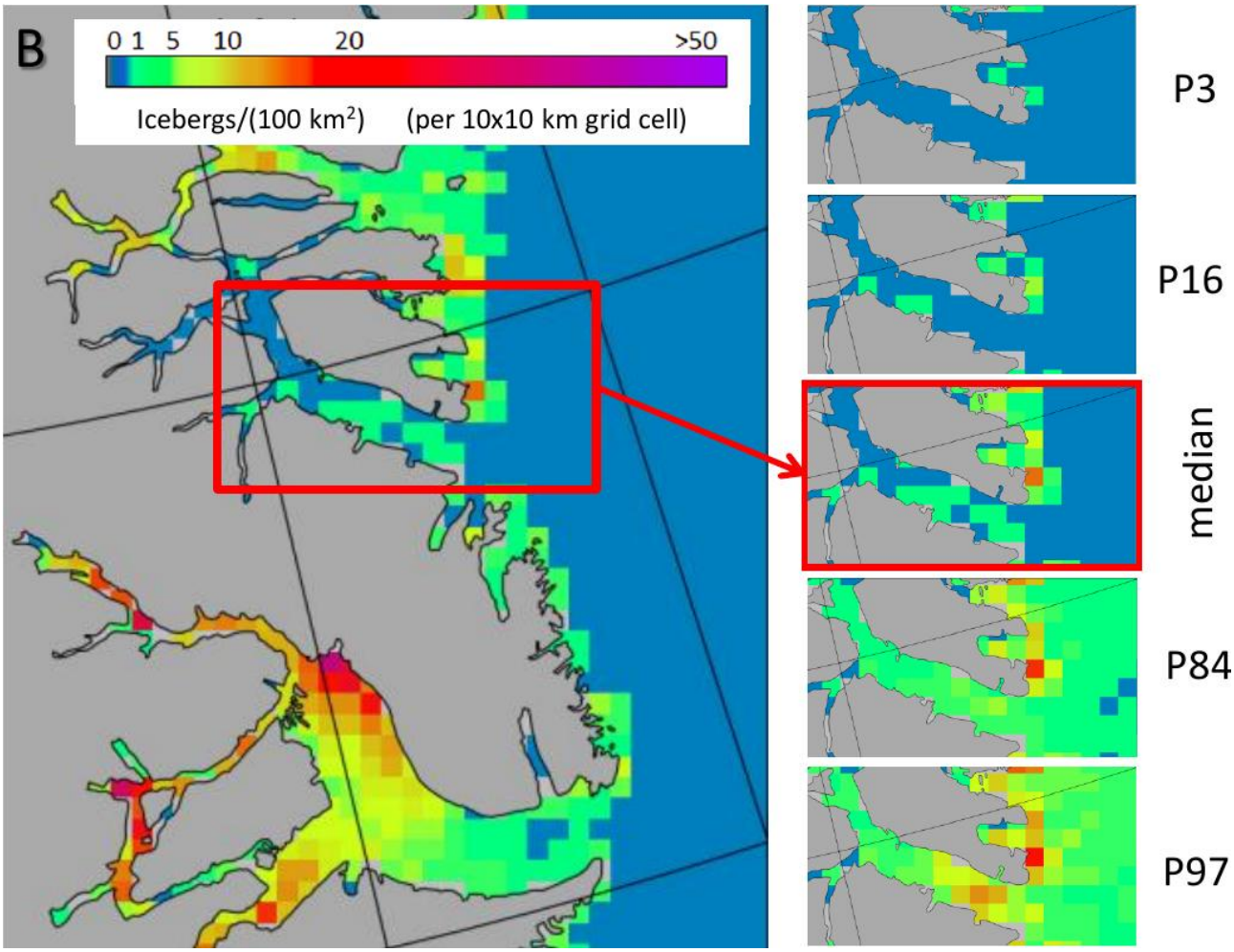

The Danish Meteorological Institute

Colophon

Serial title	DMI Report 21-43
Title	Ice and metocean conditions in and off Kong Oscar Fjord, East Greenland
Subtitle	Report for COWI
Author(s)	Mads Hvid Ribergaard and Jørgen Buus-Hinkler
Other contributors	
Responsible institution	Danish Meteorological Institute
Language	English
Keywords	Metocean, iceberg, sea ice, statistics, Greenland
URL	https://www.dmi.dk/publikationer/
Digital ISBN	978-87-7478-713-6
ISSN	2445-9127
Version	v2.0: 28 January 2022 v1.0: 23. December 2021
Website	www.dmi.dk
Copyright	Danish Meteorological Institute

The Danish Meteorological Institute

Content

The Danish Meteorological Institute

1 Abstract

In this report ice and metocean statistics is presented for Kong Oscar Fjord and surrounding sea off East Greenland. The ice statistics is based on an archive of sea ice charts and satellite detection of icebergs, whereas the metocean statistics is based on high resolution numerical models – CARRA . Finally the tides at Mestersvig is described and presented together with modelled wind driven surges.

For sea ice concentration a 22 year archive is analysed and for icebergs a 4 year archive is used. For metocean parameters 11 years of hourly data is analysed.

The following parameters is analysed and statistics for normal and extreme cases are presented as figures and charts:

Observations:
- Sea ice concentration
- Icebergs
- Tidal constituents and predictions

Model results:
- Wind speed at 10m
- Wind roses for specified locations
- Air temperature at 2m
- Visibility
- Ocean surface currents
- Sea ice drift speed
- Water level
- Ocean surface temperature
- Ocean surface salinity
- Water level and tidal analysis for Mestersvig for estimation of the wind driven part

The data-report is a visualization of the general ice and metocean condition in and off Kong Oscar Fjord as seen by DMIs model and observational products. It does not provide any conclusive considerations whether maritime operations are feasible or not. This is solely a user-dependent decision.

2 Sea ice concentration

2.1 General ice conditions off East Greenland

The ice that occurs in the waters around Greenland can be roughly divided into the following main types: multiyear ice (particularly important here), west ice (not considered here), first year/new ice and icebergs.

Multiyear ice is very heavy sea ice formed in the Arctic Ocean over more than one winter and is about 3 m thick or more. Through a process of hummocking, ice packing and subsequent freezing together, even greater thicknesses may be formed. Multiyear ice contains very little salt and almost no air bubbles, which means that it is both hard and heavy. Most of the ice within the Arctic Ocean is sooner or later exported southward through the Fram Strait between Greenland and Svalbard. From there it is drifting further south within the East Greenland Current along the entire East Greenland Coast. Thus the sea ice drifting southwards (called "Storisen" = "big ice" in Danish) within the East Greenland Current generally consists of multi-year ice from the Central Arctic and first-year ice that was formed along the Siberian coast. In addition, new-ice is constantly formed locally in polynyas and along the ice edge.

The sea ice flux trough the Fram Strait varies both seasonally and annually, and thus the volume of (particularly multiyear) ice off the East Greenland Coast changes with the seasons: Starting at a minimum in August-September, the East Greenland sea ice extent will gradually increase as winter approaches. The first part of the advancing ice mass at the beginning of winter manifests itself just off Scoresbysund and Kong Oscar Fjord approximately in October.

Typically this region does not become free of sea ice before the end of July the following year. In more severe years sea ice may be present in the region outside in Kong Oscar Fjord in all months of the year. The main challenges for navigating into the region are thus the presence of 2-3 m thick floes of multiyear ice and (infrequent) occurrence of (mainly large tabular) icebergs from the East Greenland glaciers.

Inside the East Greenland fjords the sea ice conditions is less severe since "Storisen" will seldom enter deep into the fjords, but will be transported continuously along the coast in the East Greenland Current. However, the entrance of the fjords might be blocked by "Storisen" in periods prohibiting ships to enter or leaving the fjord. The number of icebergs present inside Kong Oscar Fjord is very limited since no significant glacier outlets terminate in the fjord. Iceberg statistics is presented in chapter 3.

2.2 Ice statistics

A detailed statistics of sea ice concentration locally in Kong Oscar Fjord is given together with a general statistical overview of sea ice concentration in the Central East Greenland waters.

The Danish Meteorological Institute

Local statistics (from inside the fjord) is provided for four numbered sites going in location from the inner part (KO_1) through the central parts (KO2_, KO_3) to the mouth (KO_4) of the fjord (see map in Figure 1). The analysis is based on ice charts carried out by the Ice Service at DMI and covers 22 years from 2000 to 2021. At each of the four locations the sea ice concentration is registered in each week of the year in the 22 different years (see tables in Figure 1).

The fields in Figure 1-tables are coloured according to the World Meteorological Organisation (WMO) standard for sea ice concentration, and are thus illustrating inter-annual variations; both in the duration of the open-water season as well as in sea ice concentration at the different locations in Kong Oscar Fjord. In most years the inner parts of the fjord (KO_1, KO_2) becomes virtually free of sea ice during a continuous period ranging from two (mid-August to mid-October) to almost four (mid-July to mid-November) months, e.g. in 2008 and 2016, respectively. There is however exceptions like in 2007, where no parts of the fjord became completely free of sea ice during the summer. The outer parts of the fjord (KO_3, KO_4) are in some years characterized by the presence of sea ice (mostly in lower concentrations) interrupting the open-water season. This is most pronounced at the outermost location (KO_4) where "Storisen" sometimes may enter the outer part of the fjord like in 2020, where only two weeks (in late August) where free of sea ice at KO_4.

Figure 2 illustrates the variability in sea ice concentration offshore Central East Greenland inferred from the DMI 2000-2020 ice chart record. The figure shows the median (assumed the typical) and the extreme – low (P5) as well as high (P97) – sea ice concentrations for the months: July, August, and September.

Typically the region just off Kong Oscar Fjord and Scoresbysund becomes free of sea ice in early August. However, in extreme years "Storisen" may not leave the region at all, and the fjord may still be covered by fast ice in July. In such years accessing the fjord is more difficult. In "light" sea ice-years the whole region may, on the other hand, become ice free already in July.

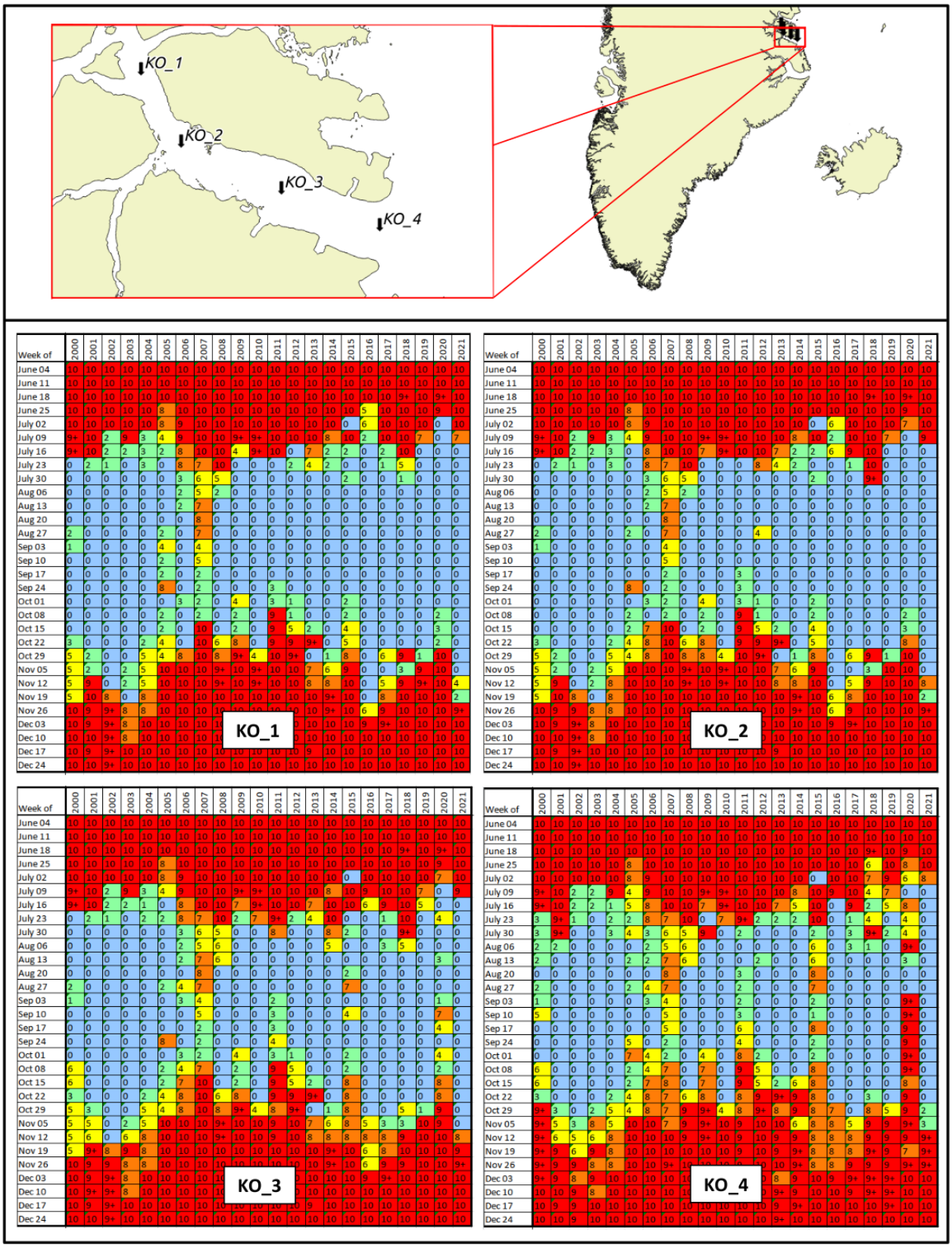

Figure 1 "Open-water-seasons" in Kong Oscar Fjord at four numbered locations going from the bottom (KO_1) through the central parts (KO2_, KO_3) to the mouth (KO_4) of the fjord. The numbers in the coloured fields indicate sea-ice concentrations in tenths.

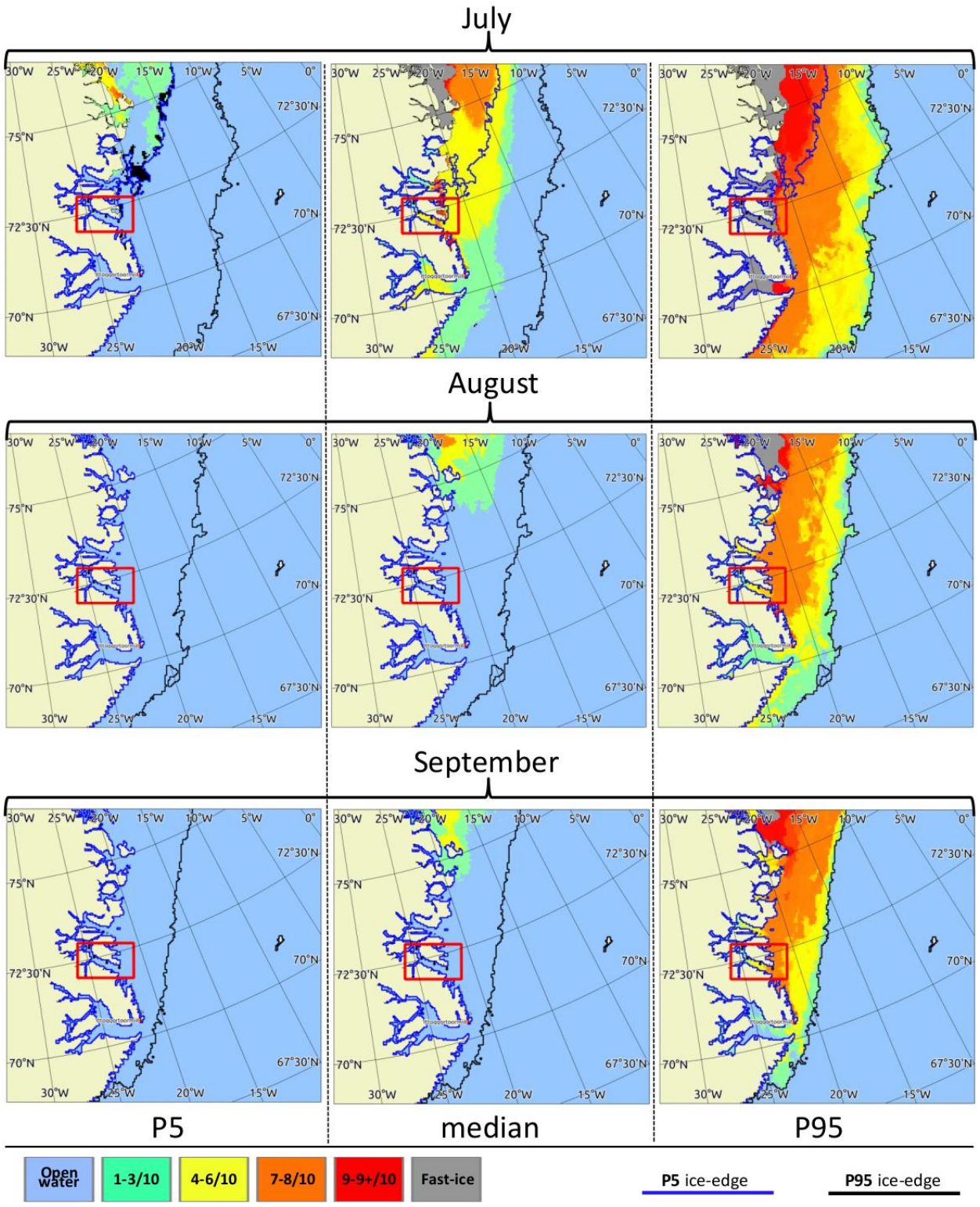

Figure 2. Regional sea ice statistics, Central East Greenland for July, August, and September derived from DMI's 21-year (2000-2020) record of ice charts. The maps show the variability in sea-ice concentration ranging from low (P5) through normal (median) to extreme (95) situations in the given months. The statistical position of the ice-edge under low (blue line) and under extreme (black line) is displayed on all maps. In the maps the red rectangle indicates the Kong Oscar Fjord Area of Interest.

3 Icebergs

The iceberg statistics given in this section is based on target (iceberg) detection in Sentinel-1 (A & B) Synthetic Aperture Radar (SAR) satellite imagery processed at the Danish Meteorological institute (DMI). Since SAR based iceberg detection in sea ice infested areas is uncertain, only iceberg-targets detected in open-water are included. The imagery that was available for the statistical analysis (2017-2020) is so called "level 1b GRDM" acquired in Extra Wide Swath mode with a spatial resolution of 60-80 m (delivered with a pixel spacing of 40 m). It shall thus be noted that the smallest icebergs + bergy bits and growlers are unlikely (or very unlikely) to be detected.

Iceberg statistics locally for Kong Oscar Fjord and the Scoresbysund Region is depicted in Figure 3 and Figure 4. Figure 3 only deals with the month of August, whereas Figure 4 gives a regional overview of the three months: July, August and September. Figure 3(A) should be regarded as a "snapshot" of the iceberg conditions in mid-August 2021 (composed of observations from August 13th, 14th, and 15th). The icebergs present in the fjord are generally quite big with an average horizontal length (as inferred from the SAR imagery) of about 200 meters. The standard deviation in length is 66 m. Note that eventual icebergs too small to be detected in the SAR imagery have not been included in the derivation of this result.

Figure 3(B) shows the "2017-2020 statistics" for mid-August (week 32). It is revealed that the numbers of icebergs present in Kong Oscar Fjord is generally at a low level compared to the other fjord systems in the region. Typically the concentration ranges from 1-5 icebergs /(100 km^2), and even under extremely high conditions numbers do not exceed about 10-12 icebergs /(100 km^2). Under very low conditions there may be virtually no icebergs present in the fjord. Figure 4 gives more or less the same picture for both July and September, although there is a tendency of a slight increase in iceberg concentration throughout the three months, however only when considering extreme (P97) conditions.

Further information on iceberg detection and iceberg distribution in the Greenland Waters can be found at the following webpages:

- http://polarportal.dk/havis-og-isbjerge/isbjerge/
- https://resources.marine.copernicus.eu/product-detail/SEAICE_ARC_SEAICE_L4_NRT_OBSERVATIONS_011_007/INFORMATION
- https://catalogue.marine.copernicus.eu/documents/PUM/CMEMS-SI-PUM-011-007.pdf
- http://ocean.dmi.dk/icebergatlas/index.php

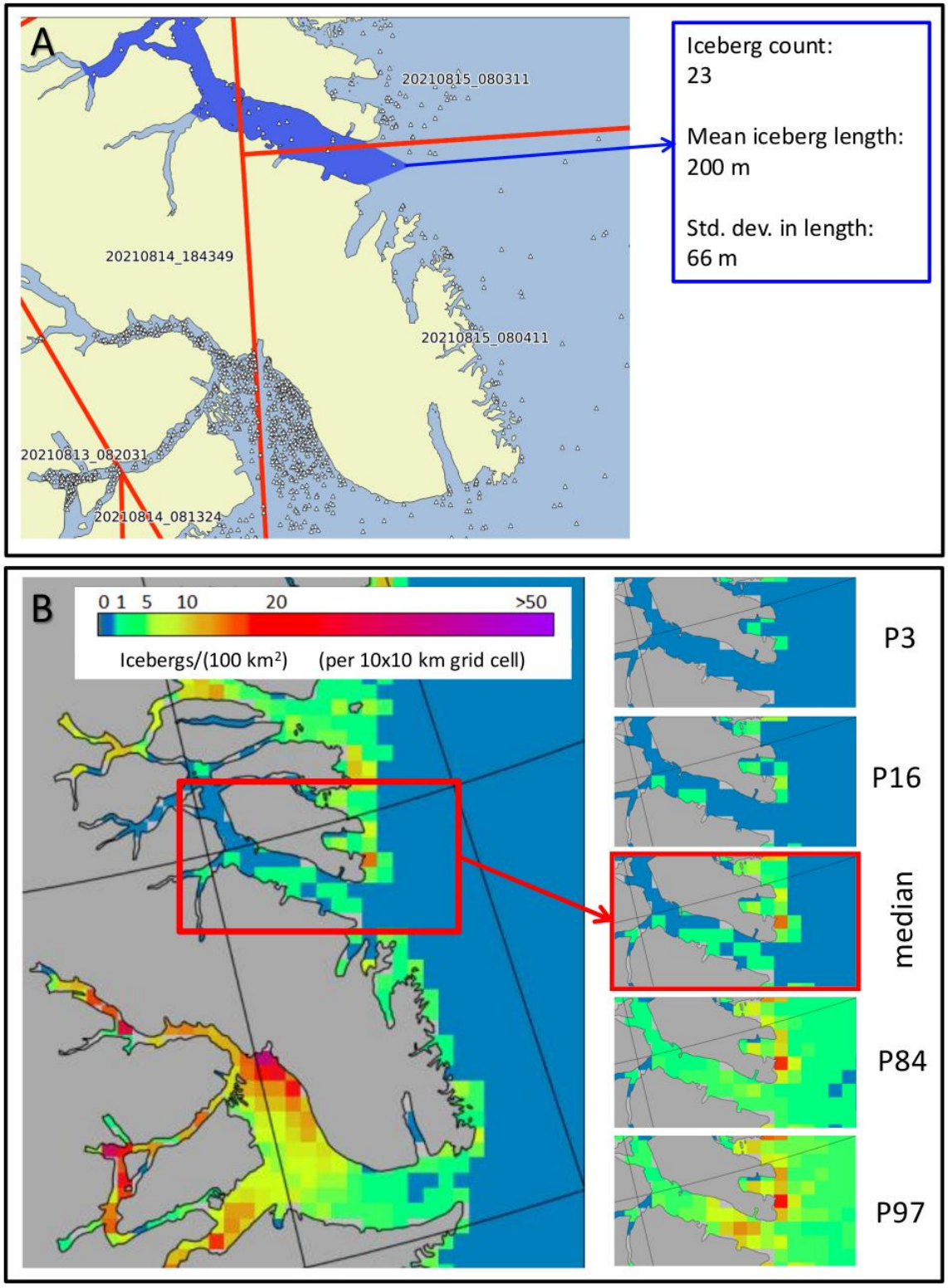

Figure 3. A: Icebergs detected with Sentinel-1 SAR satellite imagery mid-August 2021, numbers on map indicate satellite acquisition times. Red lines indicate borders between satellitite images. B: Iceberg statistics for mid-August (week 32, 2017-2020) based on iceberg detection in Sentinel-1 SAR imagery. Left: Regional map showing iceberg concentration under median (normal) conditions. Right: Iceberg concentration inside Kong Oscar Fjord under very light (P3), light (P16), normal (median), high (P84), and very high (P97) conditions.

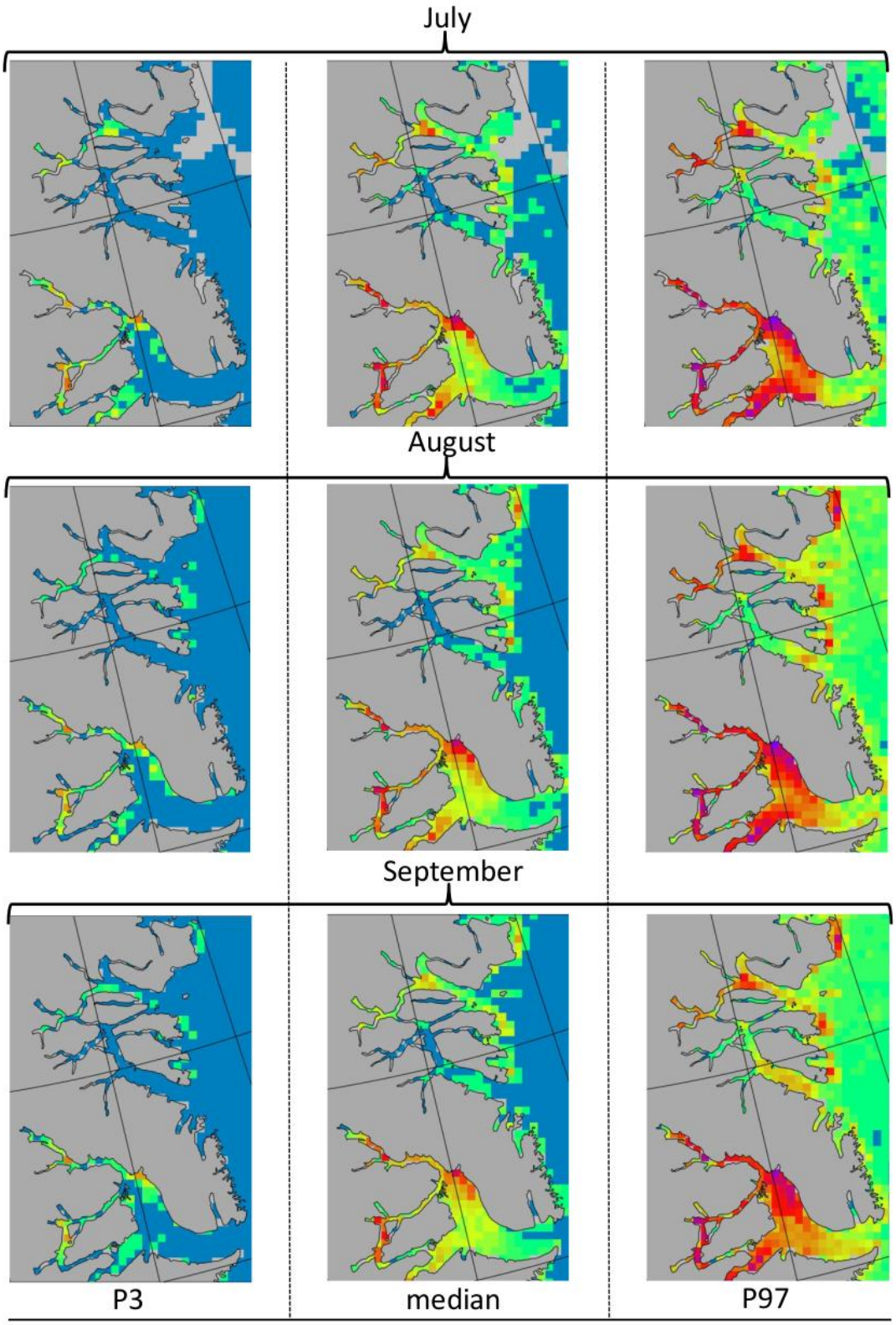

Figure 4. Regional iceberg statistics, Central East Greenland for mid-July (week 28, 2017-2020), mid-August (week 32, 2017-2020), and mid-September (week 37, 2017-2020). Iceberg concentration is shown for very light (P3) normal (median), and very high (P97) conditions. The color-coding for iceberg concentration (numbers per 10x10 km square) is the same as applied in Figure 3.

4 Meteorological statistics

In the present chapter, statistics are presented derived from the Copernicus Arctic Regional Reanalysis Service (CARRA) atmospheric reanalysis dataset (CARRA, 2021). The CARRA re-analysis is based on the HARMONIE-AROME numerical weather prediction system at a 2.5 km horizontal mesh similar to the present operational DMI-HARMONIE-IGB mesh.
As boundary forcing, it is using global reanalysis data from the global re-analysis ERA5 (Hersbach et al., 2018) at an approximately 30 km horizontal resolution.

The CARRA product provides much better local detail than the coarser resolution products of the ERA5 global reanalysis. This is especially true for the larger and deep Greenlandic fjord systems as well as the coastal winds and atmospheric conditions.

In the following statistics are given for July, August and September based on 11 years of CARRA data for the time period 2010-2021 in hourly time resolution. Statistics are given for:

- Wind speed at 10m [m/s]
- Wind roses for specified locations coloured in Beaufort scale 1-10.
- Air temperature at 2m [deg C]
- Visibility [km]

Statistics are either given as mean values, standard deviations, or percentiles where appropriate. The percentiles are obtained by sorting the data in ascending order for each grid point. The p50 percentile is identical to the median value, where 50% of the data is below, and 50% above the given value. Similar the p16 and p84 percentile separates the lowest and highest 16% of the data series. These values correspond to one standard deviation of a binomial data-distribution. Similar p03 and p97 corresponding to two times the standard deviation.

In a statistical sense, values above p84 and p97 occurs slightly less than five and one day per month respectively, but not necessary as one single event.

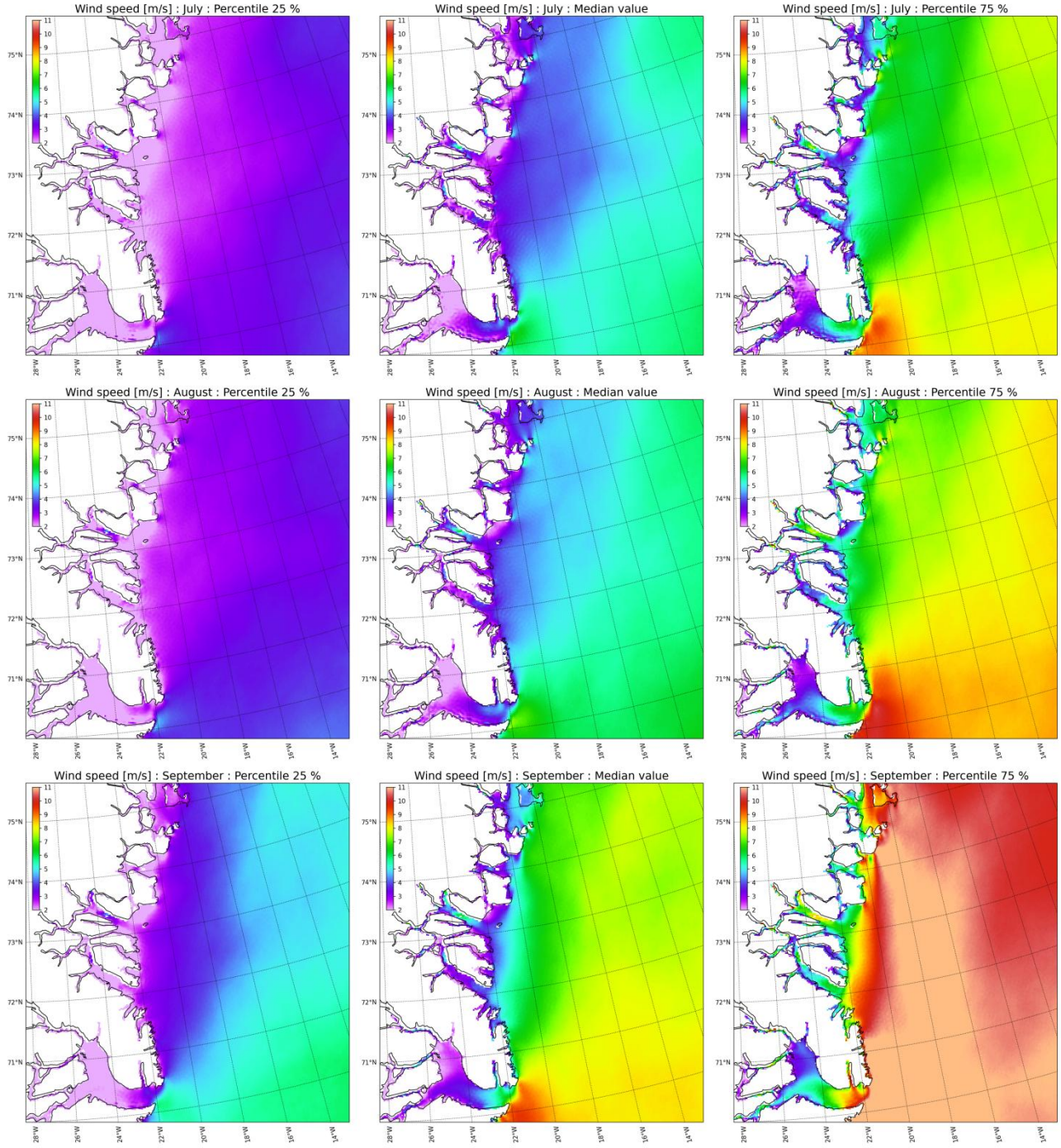

Figure 5: Wind speed statistics for July (upper), August (middle) and September (lower) based on 11 years (2010-2020) of CARRA atmospheric reanalysis valid 10m above surface. From left to right: 25%, 50% and 75% percentile.

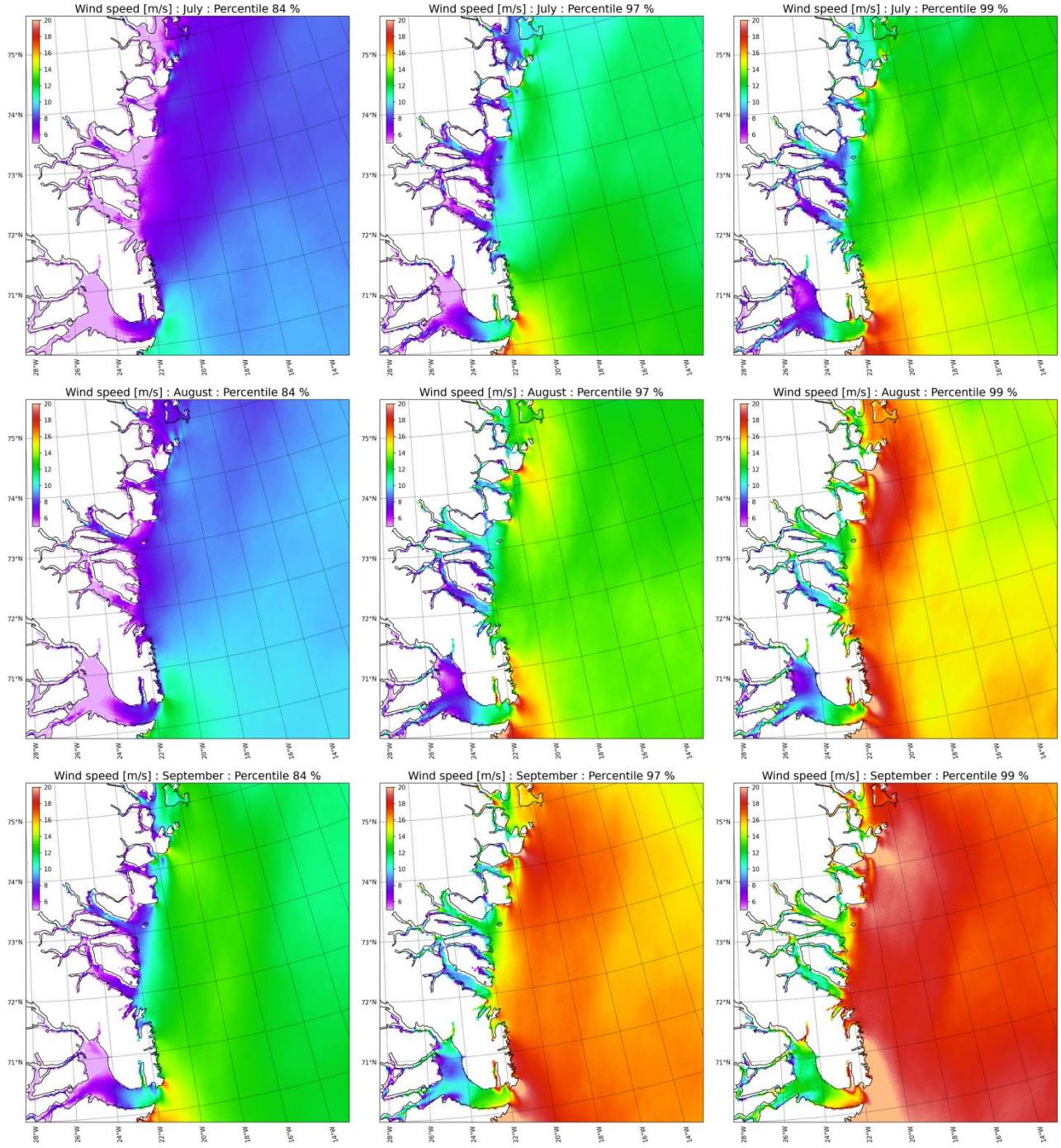

Figure 6: Wind speed statistics for July (upper), August (middle) and September (lower) based on 11 years (2010-2020) of CARRA atmospheric reanalysis valid 10m above surface. From left to right: 84%, 97% and 99% percentile.

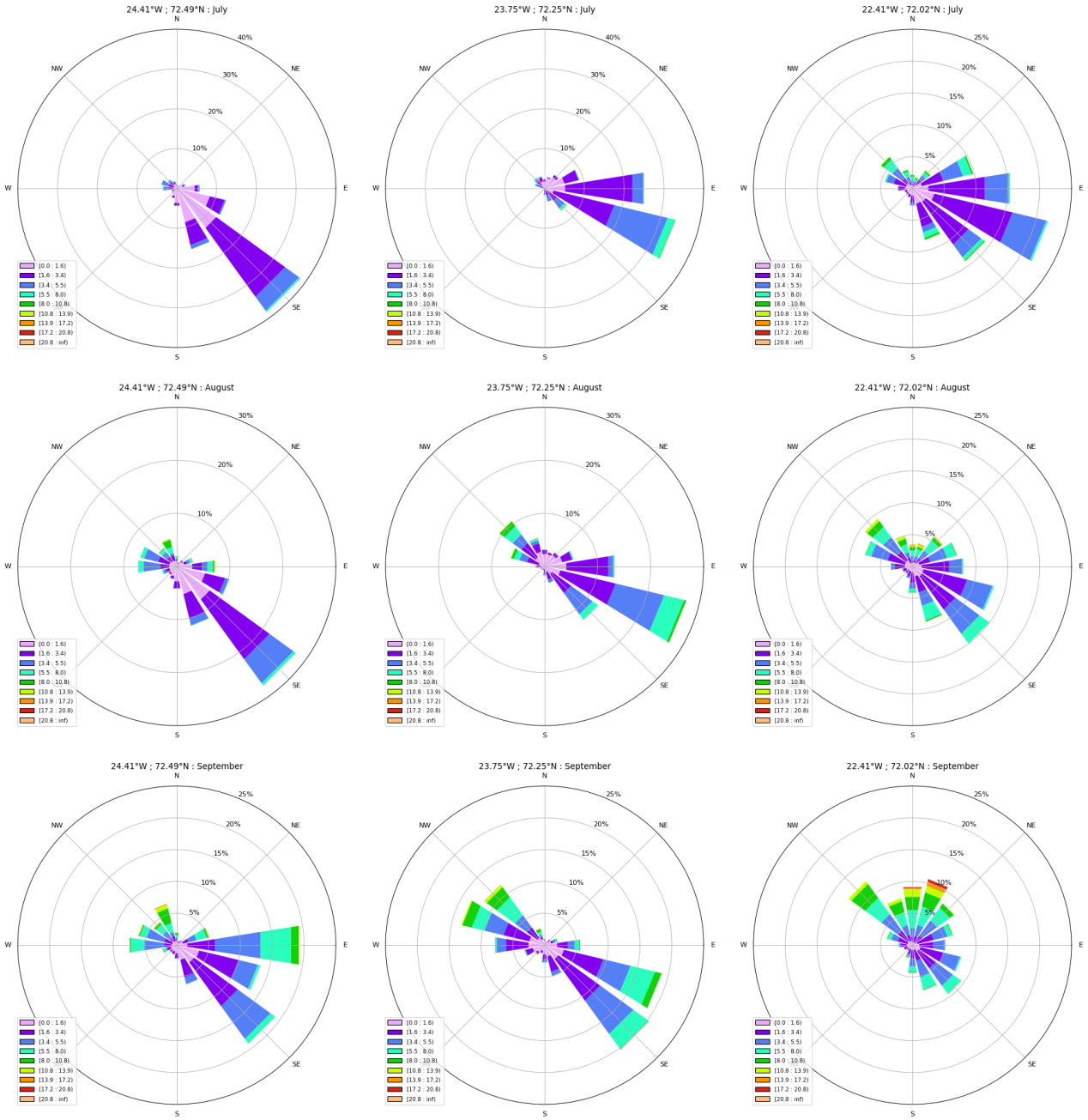

Figure 7: Wind roses for July (upper), August (middle) and September (lower) based on 11 years (2010-2020) of CARRA atmospheric reanalysis valid 10m above surface. Colour scale corresponds to Beaufort scale 1-9. From left to right: Approximately position KO_2, KO_3 (Mestersvig) and KO_4 as shown in Figure 1.

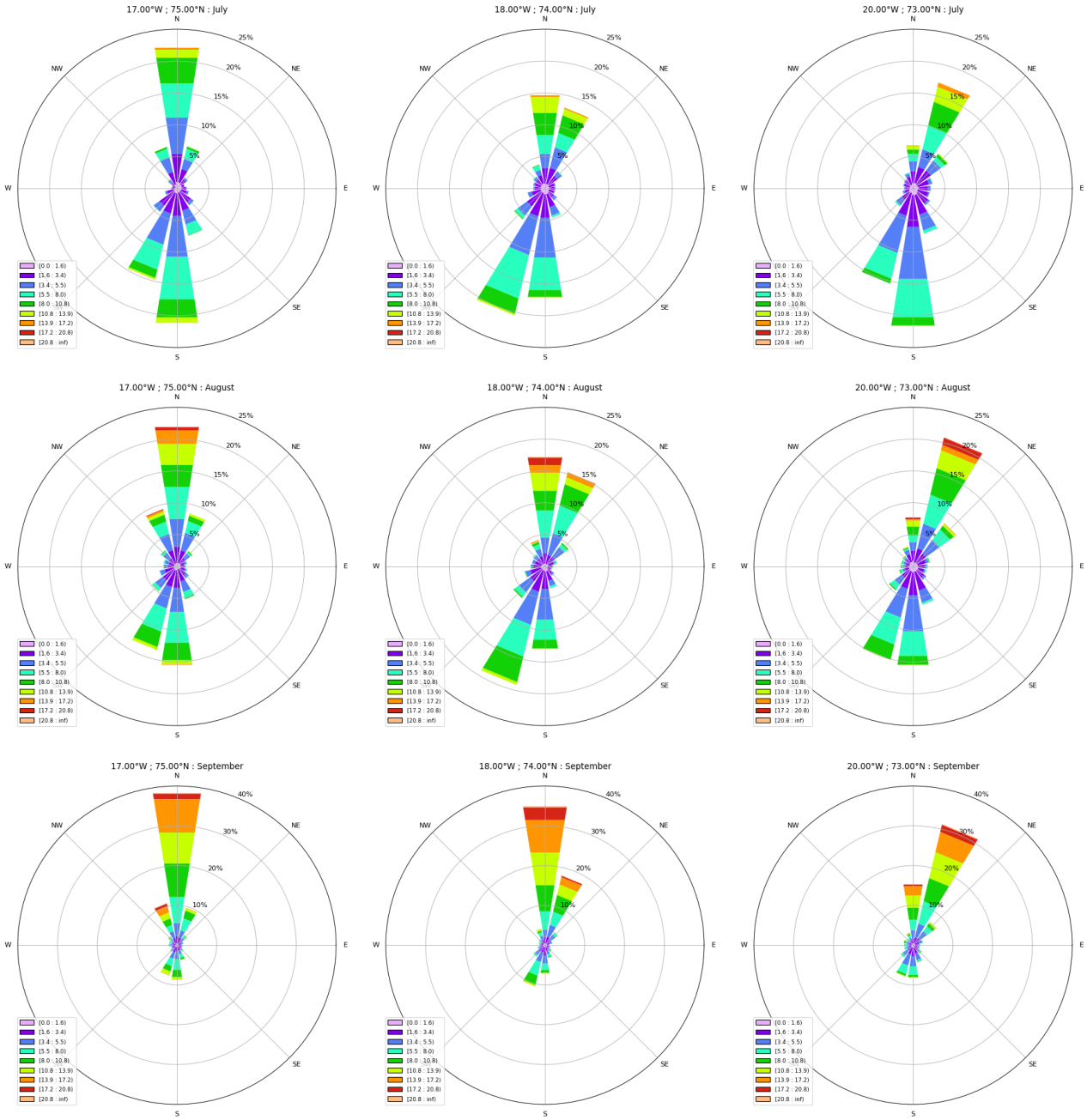

Figure 8: Wind roses for July (upper), August (middle) and September (lower) based on 11 years (2010-2020) of CARRA atmospheric reanalysis valid 10m above surface. Colour scale corresponds to Beaufort scale 1-9. From left to right: Coastal locations at 75N, 74N and 73N.

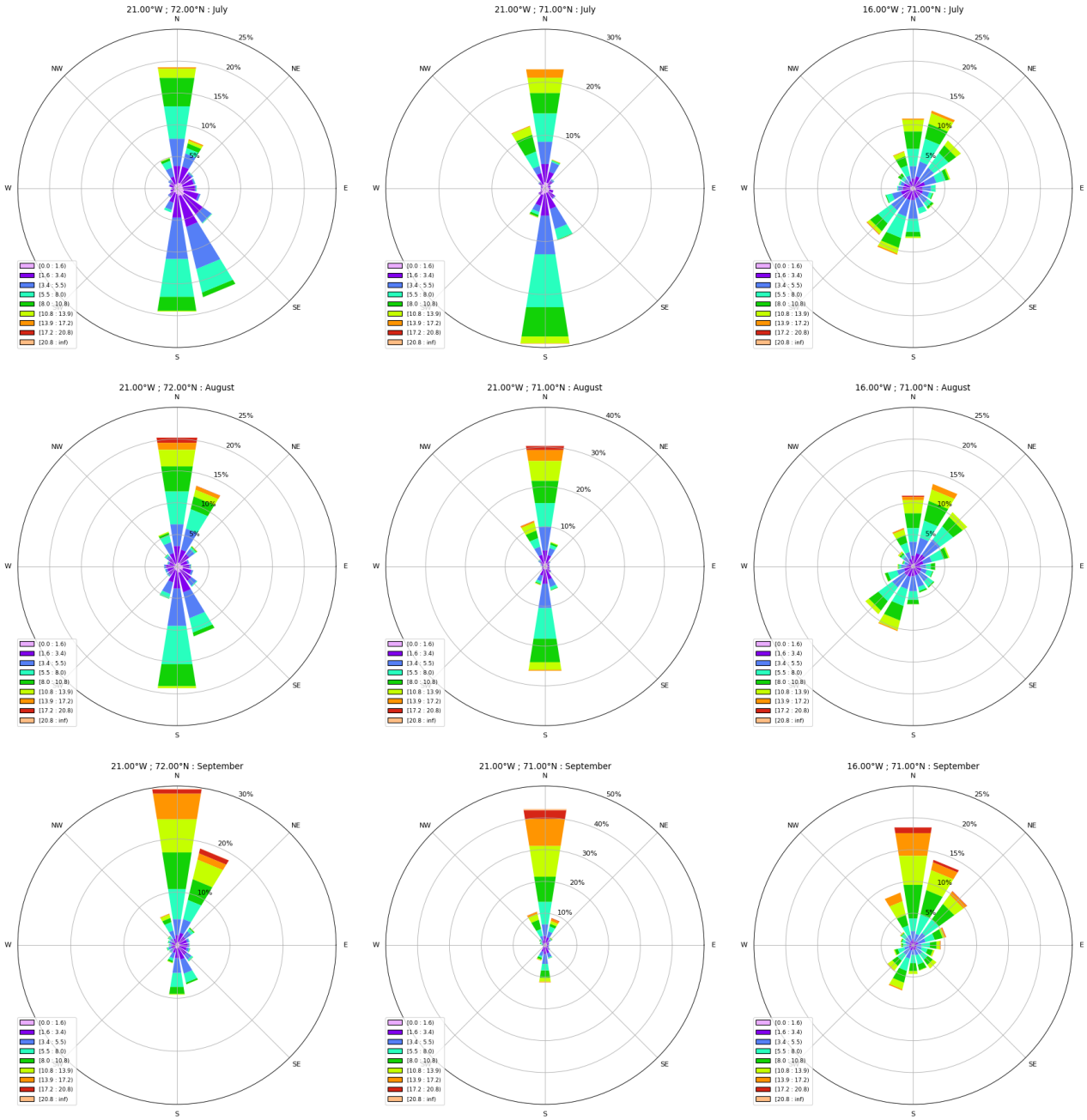

Figure 9: Wind roses for July (upper), August (middle) and September (lower) based on 11 years (2010-2020) of CARRA atmospheric reanalysis valid 10m above surface. Colour scale corresponds to Beaufort scale 1-9. From left to right: Coastal locations at 72N, 71N and offshore 71N.

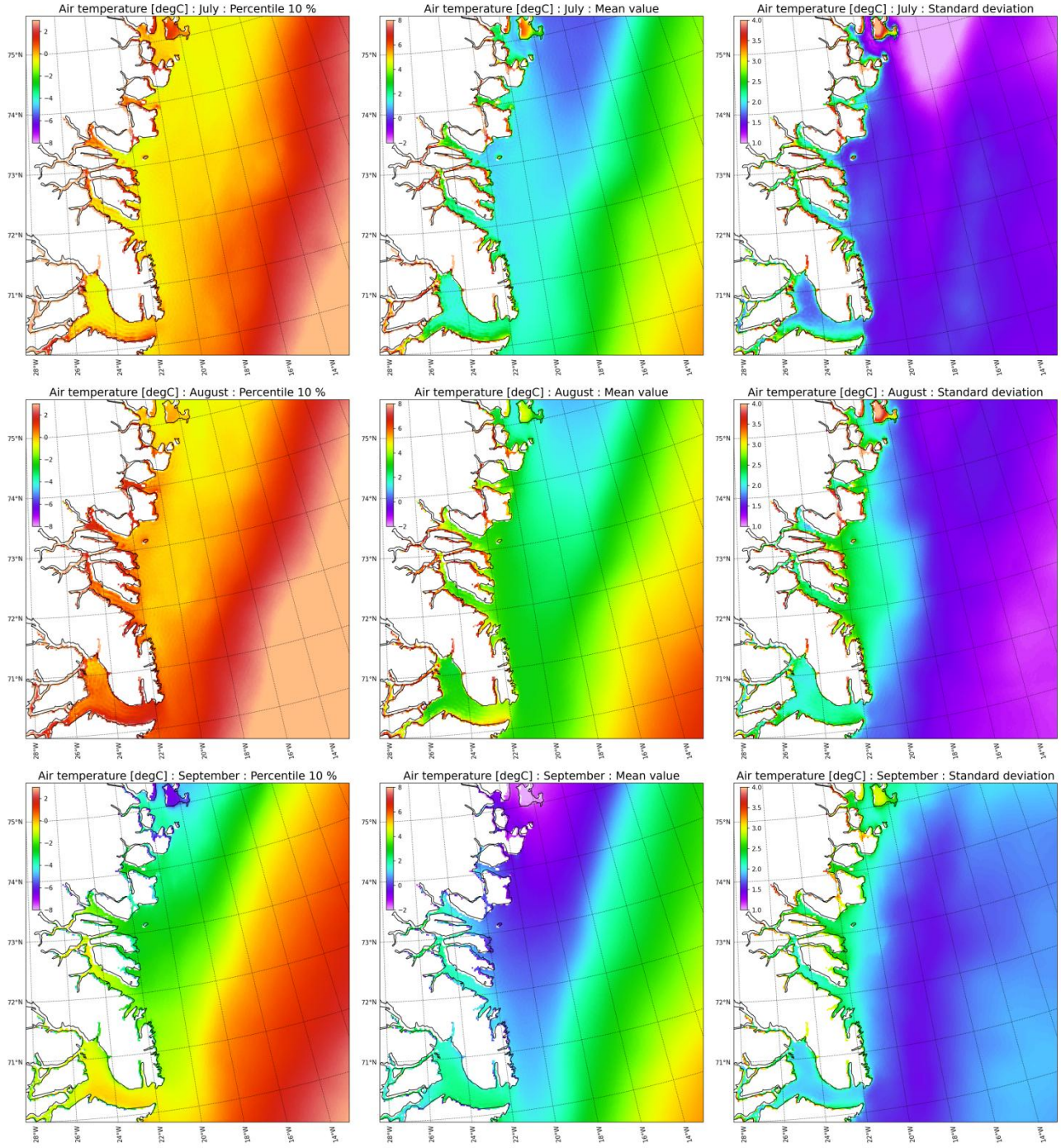

Figure 10: Air temperature statistics for July (upper), August (middle) and September (lower) based on 11 years (2010-2020) of CARRA atmospheric reanalysis valid 2m above surface. From left to right: 10%, percentile, mean value and standard deviation.

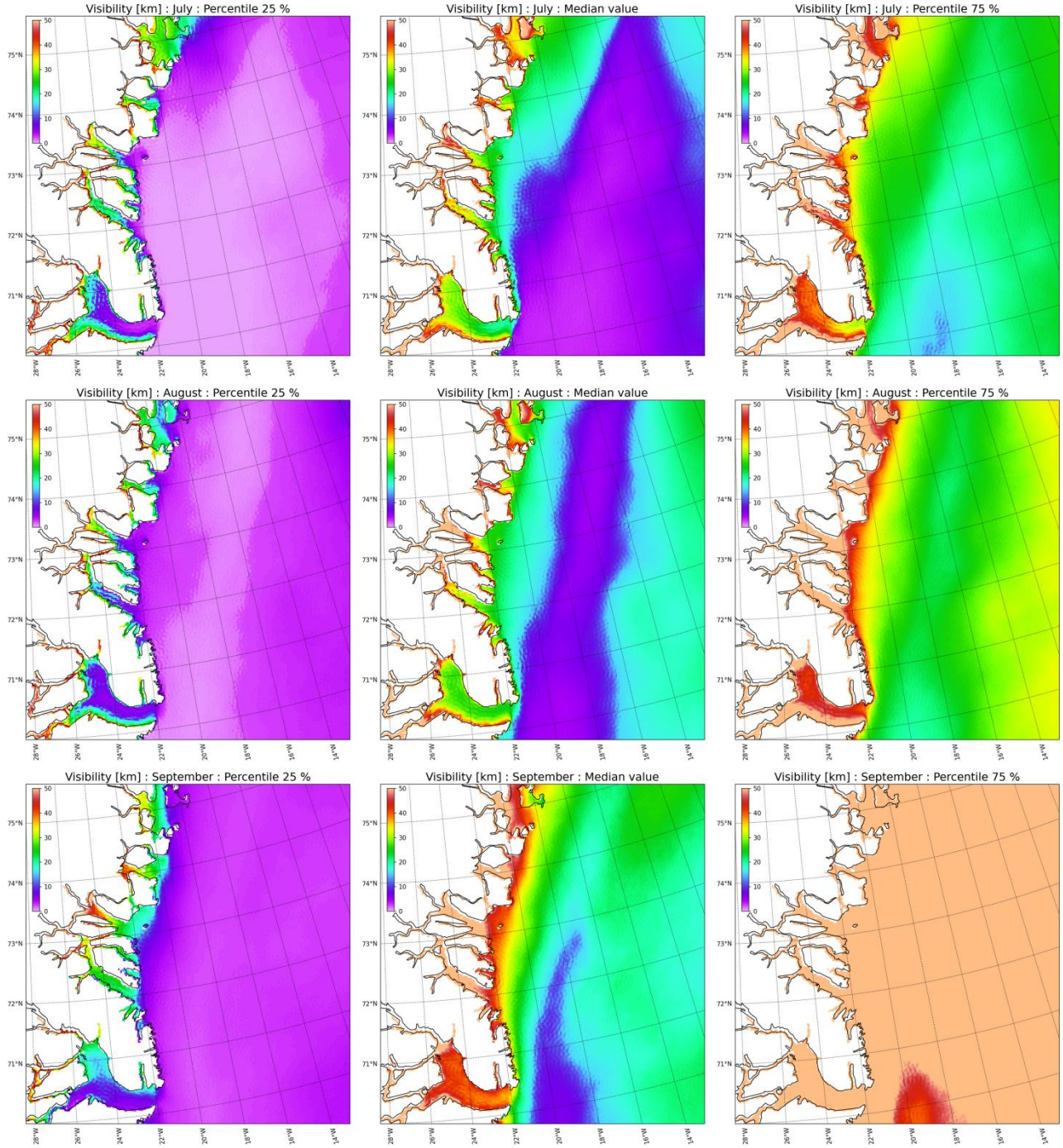

Figure 11: Surface visibility statistics for July (upper), August (middle) and September (lower) based on 11 years (2010-2020) of CARRA atmospheric reanalysis. From left to right: 25%, median value and 75% percentiles.

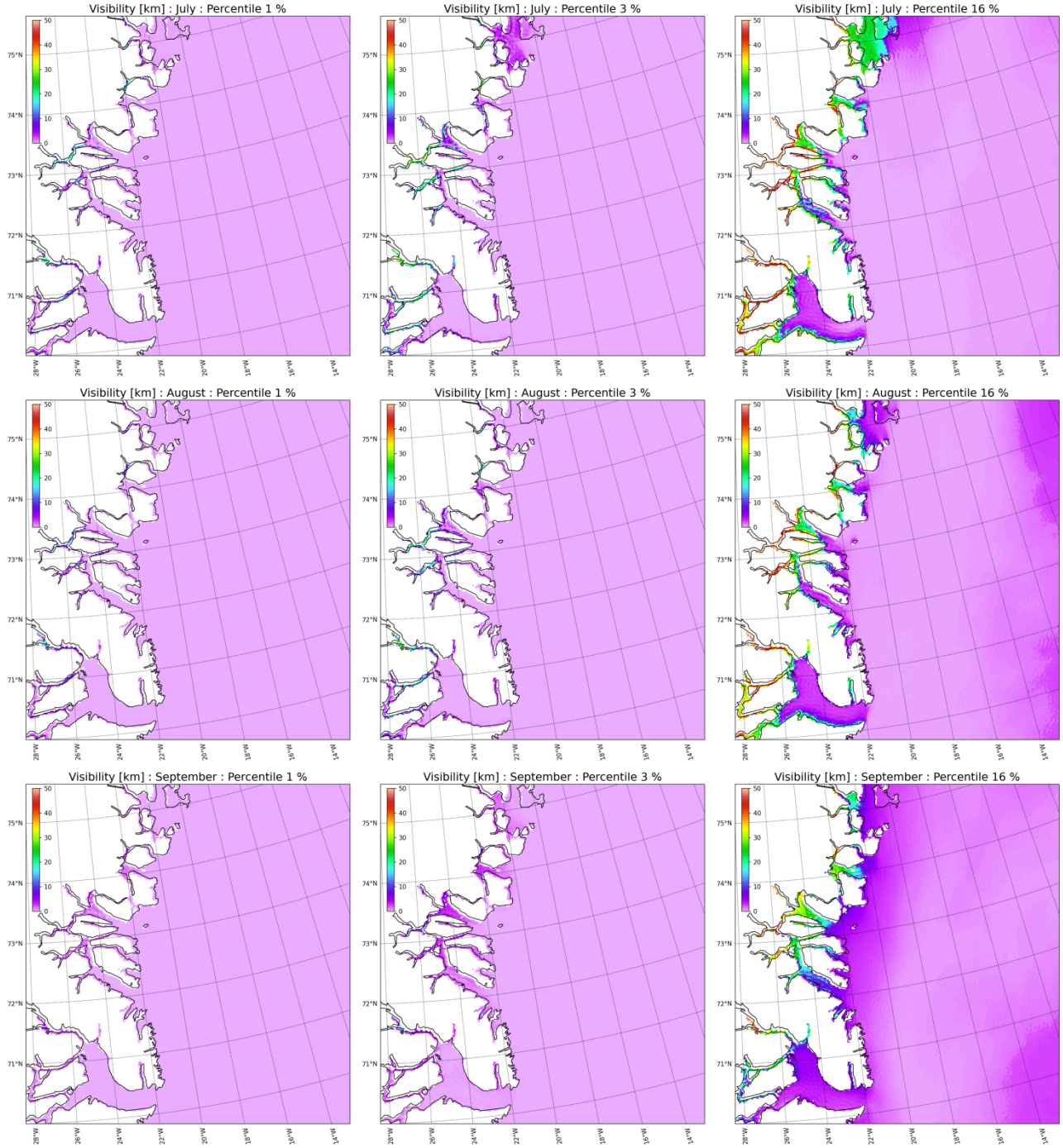

Figure 12: Surface visibility statistics for July (upper), August (middle) and September (lower) based on 11 years (2010-2020) of CARRA atmospheric reanalysis. From left to right: 1%, 3% and 16% percentiles.

5 Ocean surface statistics

DMI is running an operational ocean- and sea-ice model for the Arctic Ocean and Atlantic Ocean with focus on Greenland. HYCOM-CICE is a fully coupled ocean- and sea ice model system, which has recently undergone a major update.

The components of the model system are the ocean model HYCOM (Metzger et al, 2014), the sea ice model CICE (Hunke et al., 2020, 2021) and ESMF coupler (Hill et al, 2014). The system covers the area from 20° south and includes the North Atlantic and the Arctic Ocean.

The resolution is about 5 km in the Arctic and the Greenlandic waters and coarser towards south to about 10 km, away from our focus area. It does partly resolve the largest fjords in Greenland including Kong Oscar Fjord at a 5 km resolution.

The fresh water discharges from Greenland has been updated (Mankoff et al., 2020). This has the effect, that the coastal currents around Greenland are now much better represented. The extra fresh water supply lowers the coastal salinities and thereby increases the baroclinic coastal currents. Thereby the southward sea ice transport along the East Greenland coast is speeding up and comes closer to the coast in better agreement with observations. The model setup assimilates towards the same satellite products for sea surface temperature and sea ice concentration

The model run started with a long simulation using ERA5 reanalysis atmospheric forcing (Hersbach et al., 2018) from September 1990 until 2019, and thereafter deterministic 8 km ECMWF atmospheric forcing (Haiden et al., 2021). The first 10 years until 2000 is considered as a spin-up period of the model system in order to build up a correctly represented sea ice cover and spin-up of the upper ocean surface.

In the following statistics are given for July, August and September based on 11 years of HYCOM_CICE data for the time period 2010-2021 in hourly time resolution. Statistics are given for:

- Surface current speed [cm/s]
- Sea ice drift speed [cm/s]
- Water level [m]
- Ocean surface temperature [degC]
- Ocean surface salinity [psu]

Water level data is displayed relative to local zero, expect for “mean value”, which is relative to chart mean (Figure 17 and Figure 18). The latter clearly reflects the lower density waters near the coast and the mean southward water transport.

Statistics is either given as mean values, standard deviations, or percentiles where appropriate. The percentiles are obtained by sorting the data in ascending order for each grid point. The p50 percentile is identical to the median value, where 50% of the data is below, and 50% above the given value. Similar the p16 and p84 percentile separates the lowest and highest 16% of the data series. These values correspond to one standard deviation of a binomial data-distribution. Similar p03 and p97 corresponding to two times the standard deviation. In a statistical sense, values above

p84 and p97 occurs slightly less than five and one day per month respectively, but not necessary as one single event.

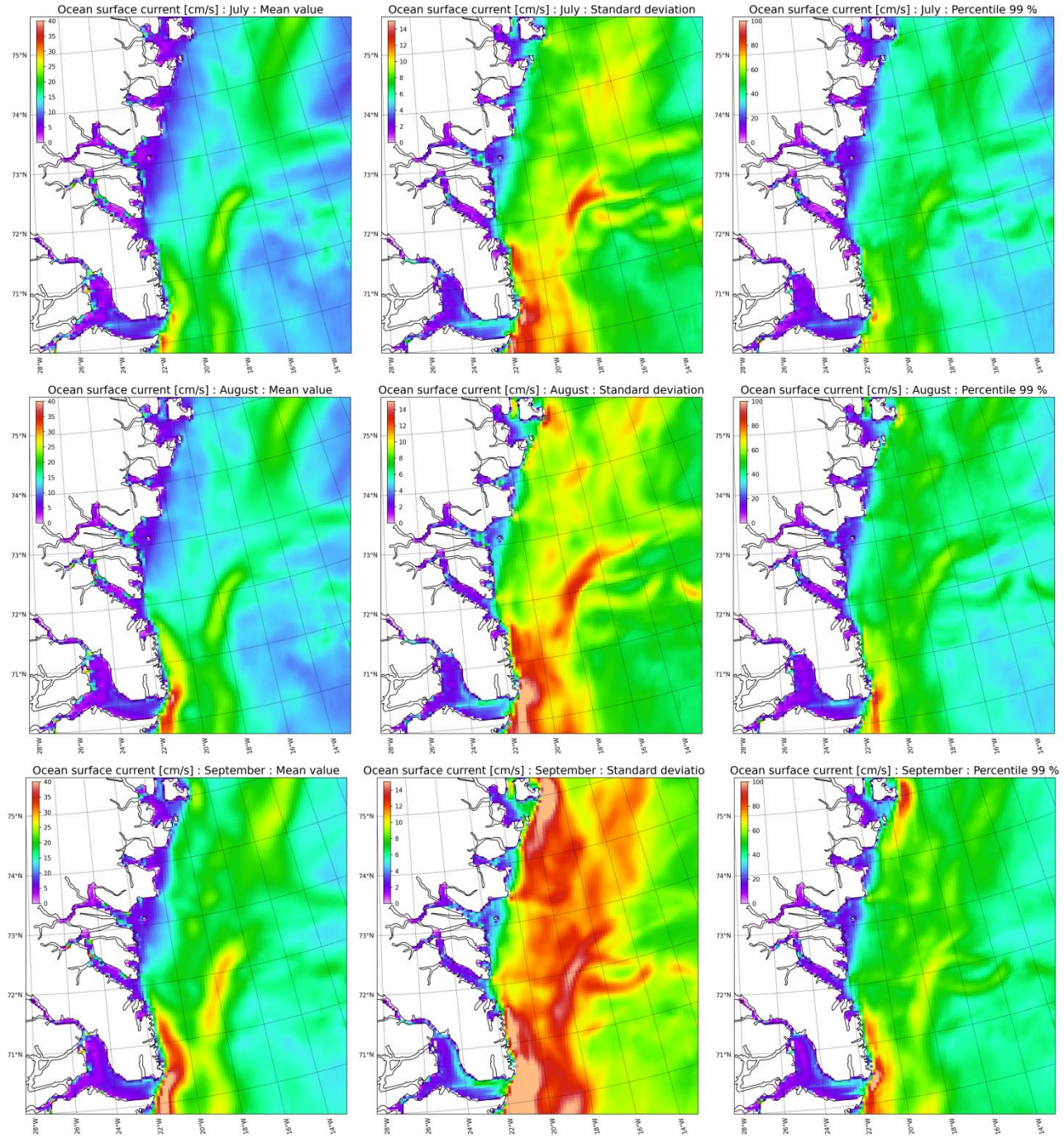

Figure 13: Ocean surface current speed [cm/s] statistics for July (upper), August (middle) and September (lower) based on 11 years (2010-2020) of HYCOM_CICE model simulation. From left to right: Mean, standard deviation and 99% percentile.

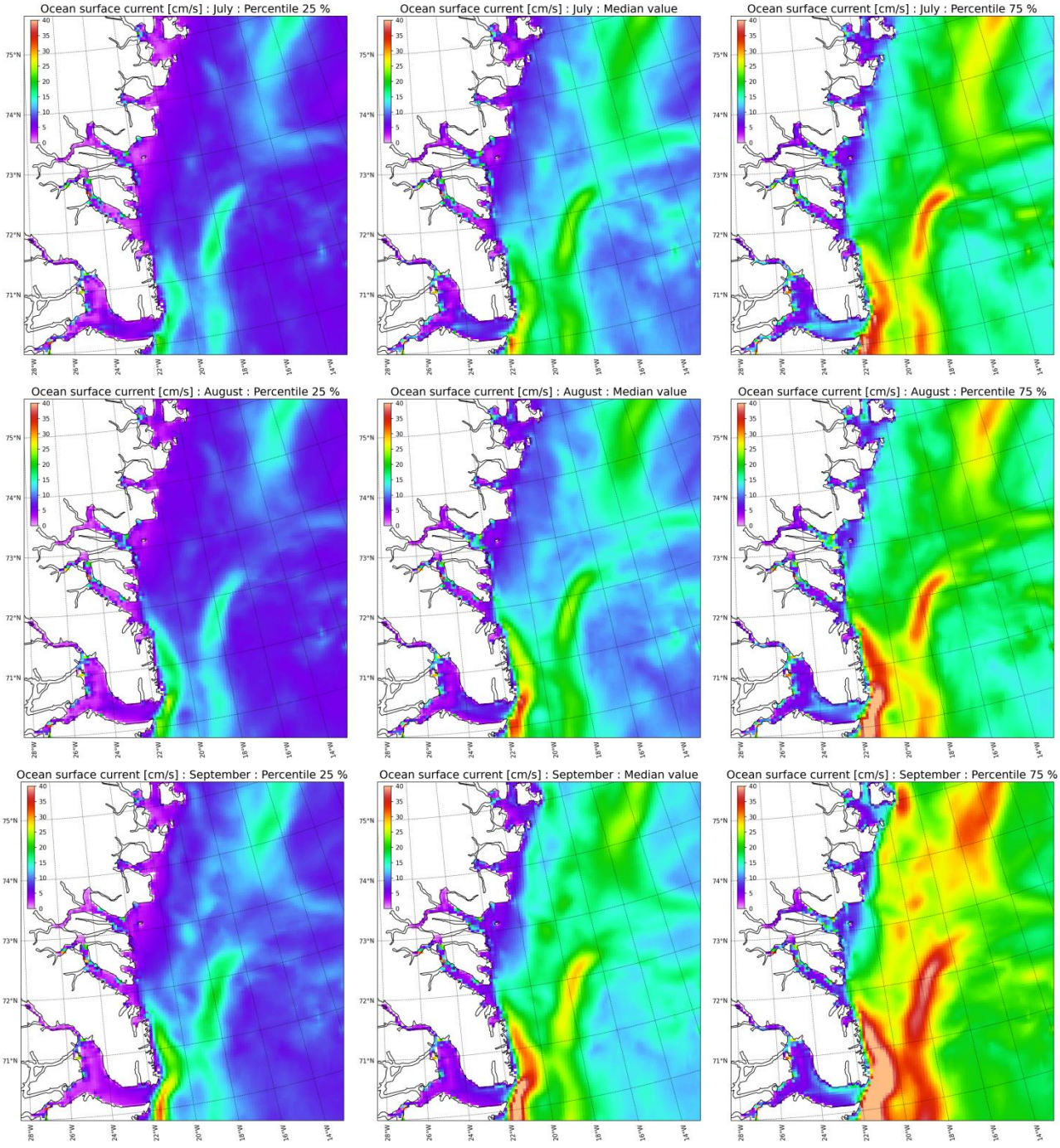

Figure 14: Ocean surface current speed [cm/s] statistics for July (upper), August (middle) and September (lower) based on 11 years (2010-2020) of HYCOM_CICE model simulation. From left to right: 25% percentile, median value and 99% percentile.

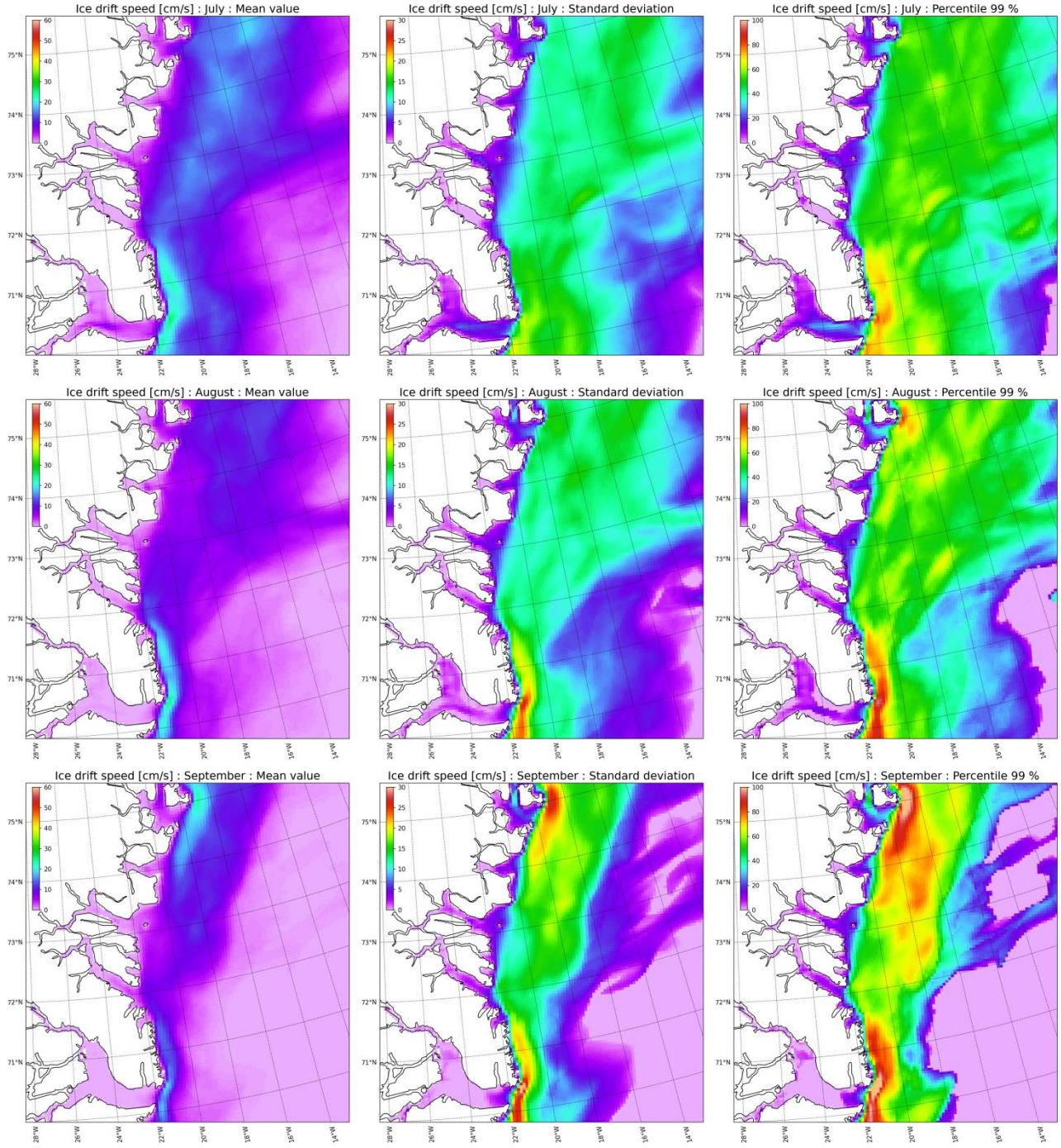

Figure 15: Sea-ice drift speed [cm/s] statistics for July (upper), August (middle) and September (lower) based on 11 years (2010-2020) of HYCOM_CICE model simulation. From left to right: Mean, standard deviation and 99% percentile.

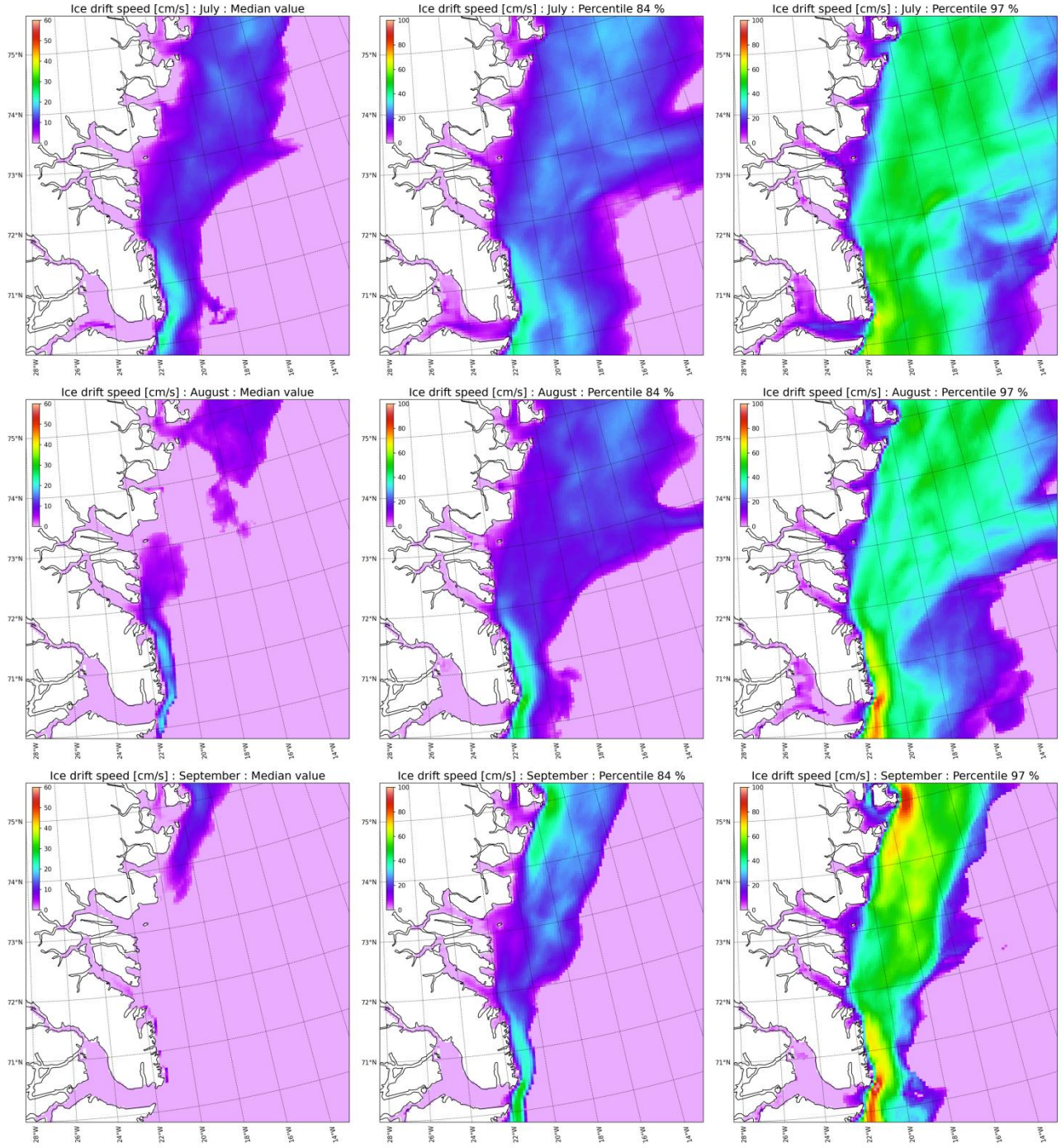

Figure 16: Sea-ice drift speed [cm/s] statistics for July (upper), August (middle) and September (lower) based on 11 years (2010-2020) of HYCOM_CICE model simulation. From left to right: median value, 84% and 99% percentile.

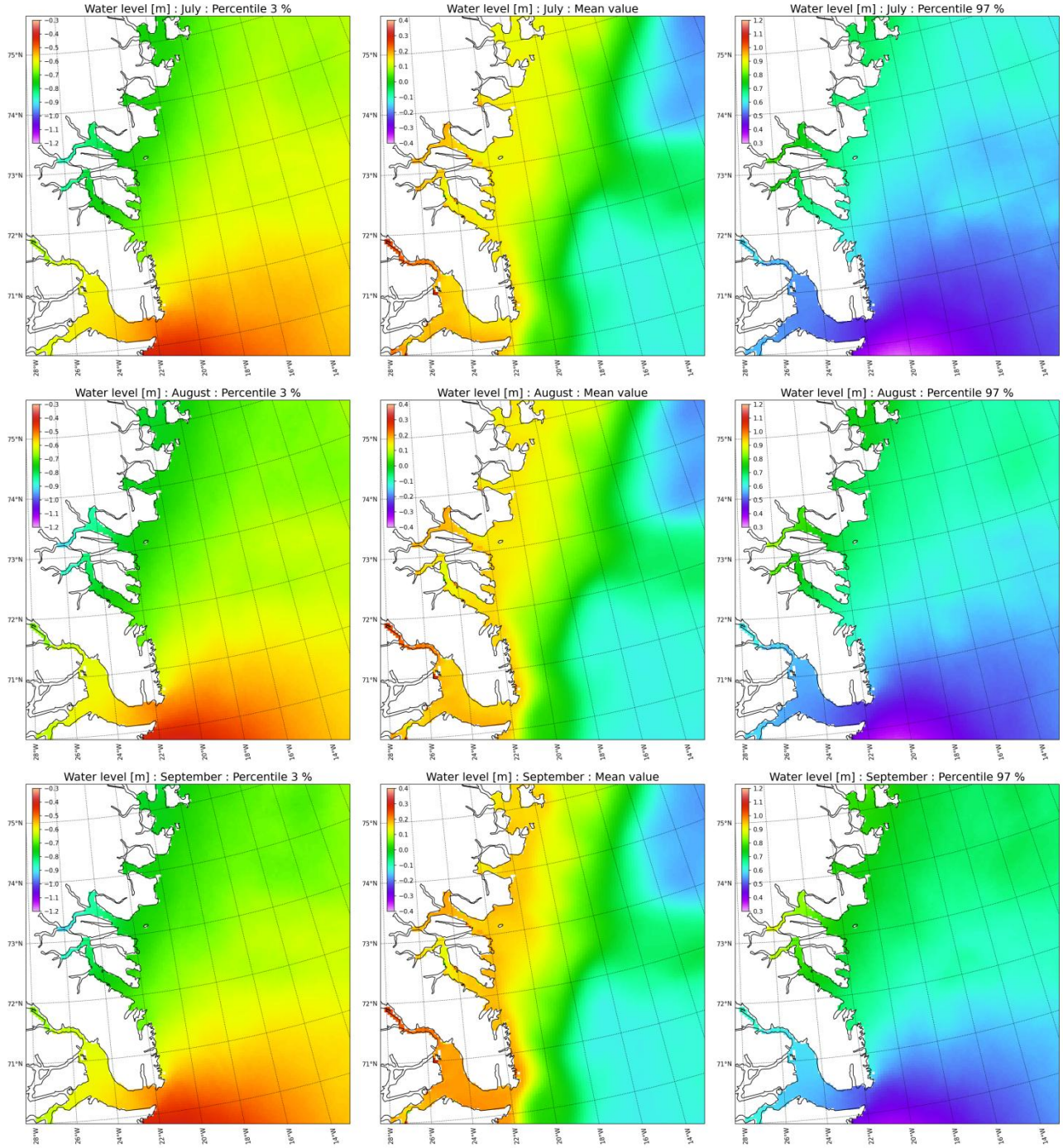

Figure 17: Sea surface height [m] statistics for July (upper), August (middle) and September (lower) based on 11 years (2010-2020) of HYCOM_CICE model simulation. From left to right: 3% percentile, mean value and 97% percentile. NOTE: Water levels are relative to local zero, except for "mean value", which is relative to the chart mean.

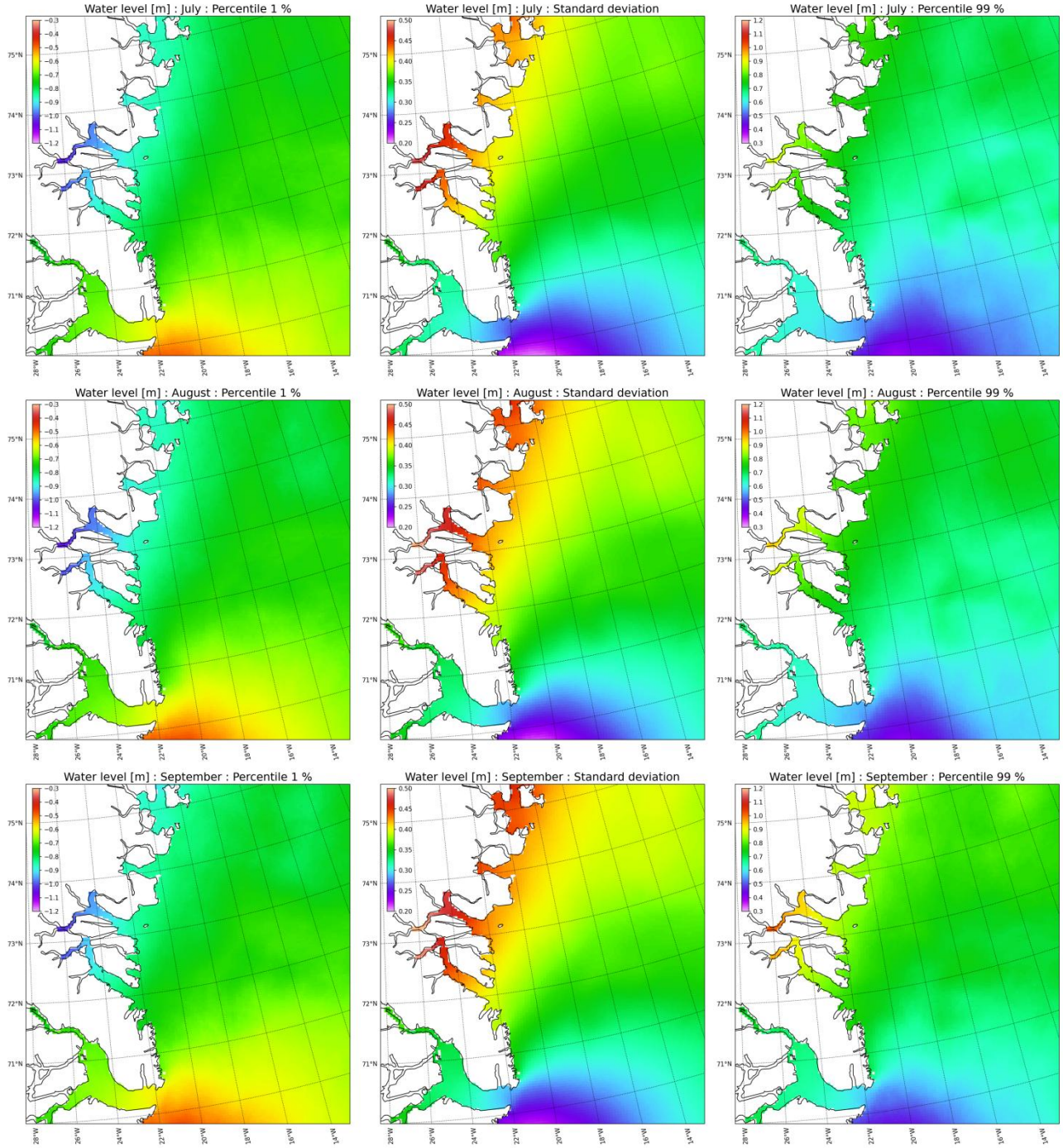

Figure 18: Sea surface height [m] statistics for July (upper), August (middle) and September (lower) based on 11 years (2010-2020) of HYCOM_CICE model simulation. From left to right: 1% percentile, standard deviation and 99% percentile. NOTE: Water levels are relative to local zero, except for "mean value", which is relative to the chart mean.

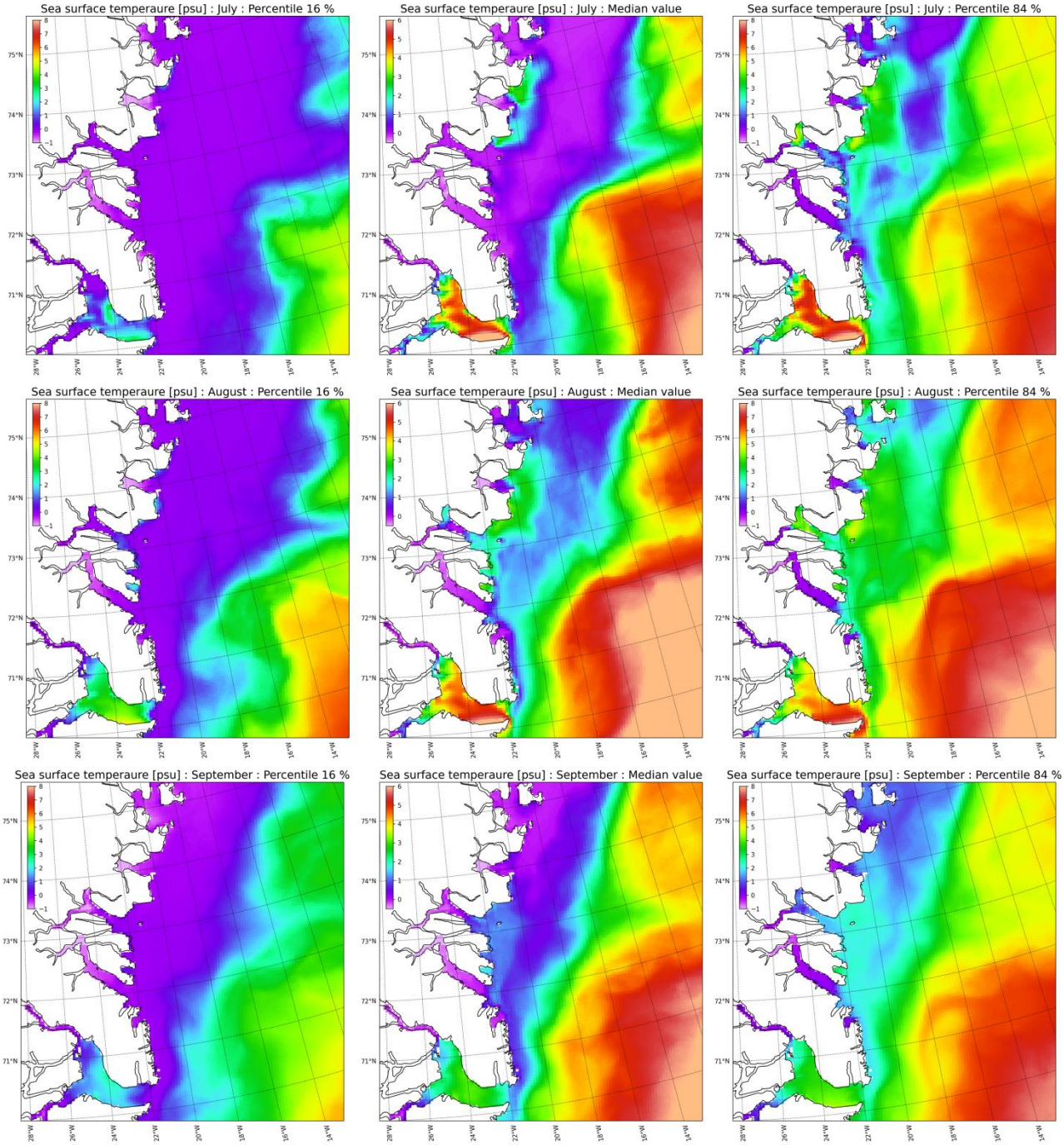

Figure 19: Sea surface temperature [deg C] statistics for July (upper), August (middle) and September (lower) based on 11 years (2010-2020) of HYCOM_CICE model simulation. From left to right: 16% percentile, median value and 84% percentile.

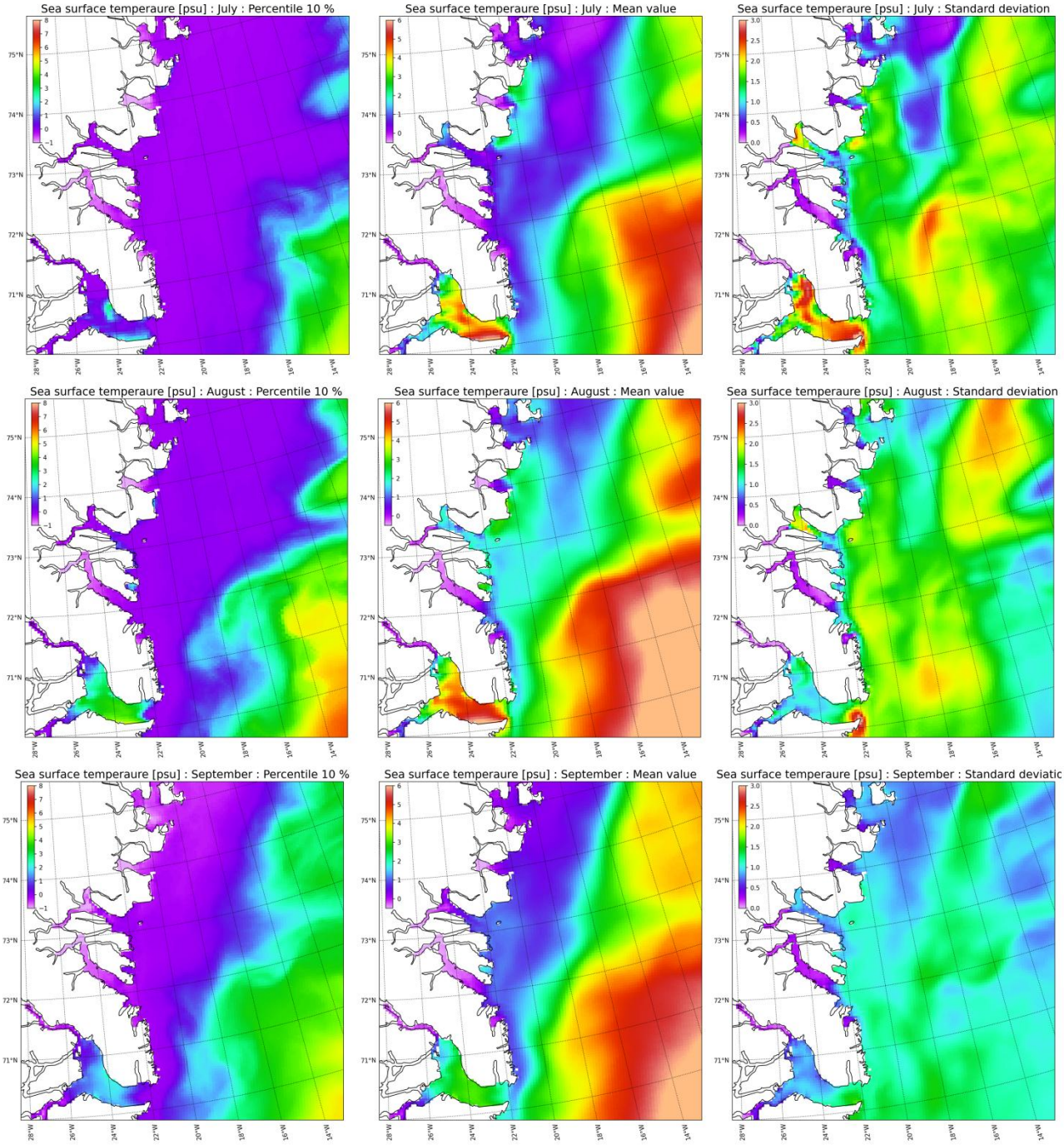

Figure 20: Sea surface temperature [deg C] statistics for July (upper), August (middle) and September (lower) based on 11 years (2010-2020) of HYCOM_CICE model simulation. From left to right: 10% percentile, mean value and standard deviation.

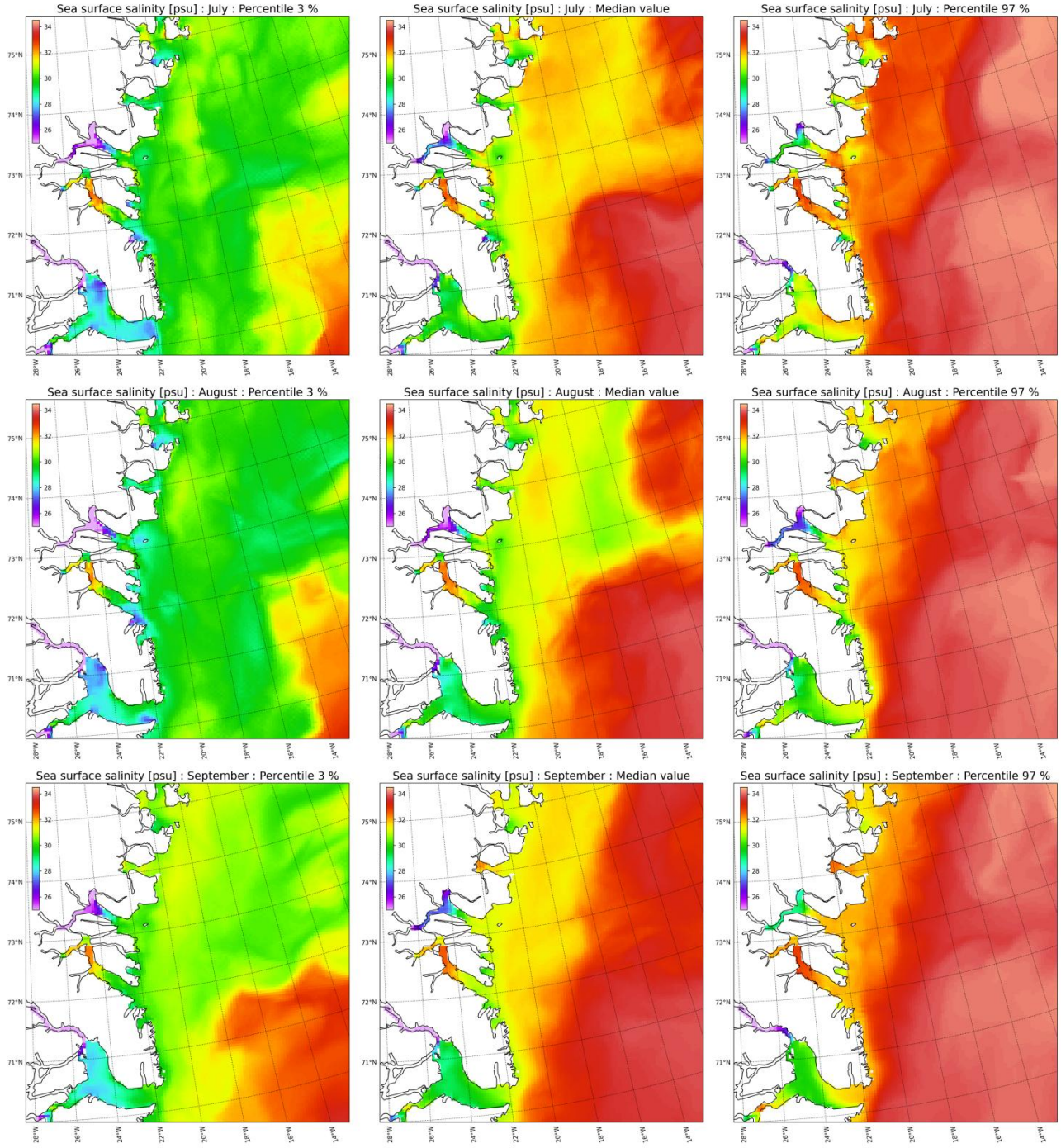

Figure 21: Sea surface salinity [psu] statistics for July (upper), August (middle) and September (lower) based on 11 years (2010-2020) of HYCOM_CICE model simulation. From left to right: 3% percentile, median value and 97% percentile.

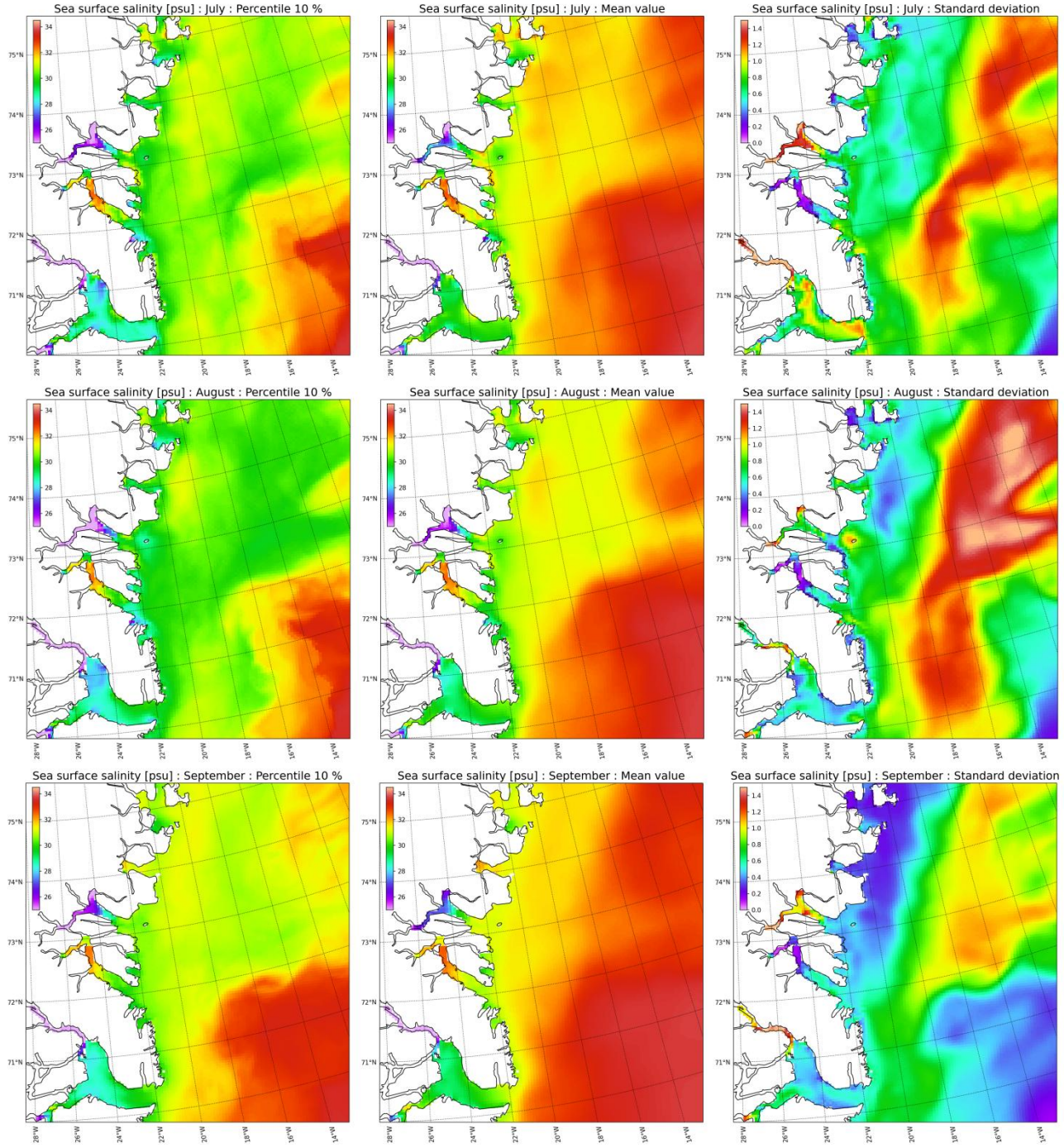

Figure 22: Sea surface salinity [psu] statistics for July (upper), August (middle) and September (lower) based on 11 years (2010-2020) of HYCOM_CICE model simulation. From left to right: 10% percentile, mean value and standard deviation.

6 Tidal water level statistics

Tides in Greenlandic waters are semidiurnal with a significant 14-days cycle, where the spring tide (around new and full moon) is a factor of 2-3 larger than the nip tide (at crescent moon). In addition, the tide also exhibits a large daily inequality as the three major characteristics. The tides are generally very strong with a maximum tidal ranges above 5 meters at Nuuk in West Greenland, where the tides is strongest. At the east coast the tidal ranges is less, but still significant and the major characteristics describing the water levels.

At Mestersvig, inside Kong Oskars Fjord, a set of tidal constituents exists based on old water level recordings of unknown origin and quality (Table 1). However, there is no reason not to trust the tidal analysis, which is assumed to be correct. Tidal prediction based on these constituents is shown in Figure 23a.

Table 1: Tidal constituents for Mestersvig. Analysis and source data is of unknown origin

Constituent	Amplitude [cm]	Phase [degrees]
O1	8.2	59.8
P1	3.6	104.9
K1	11.0	105.1
N2	11.2	345.3
M2	44.5	1.0
S2	18.4	44.0
K2	5.0	44.2
M4	1.3	58.9
MS4	1.2	95.0

The lowest and highest astronomical tide (LAT and HAT), is calculated to be -90.9 cm and +82.5 cm respectively, based on the 19 year time period 19970101–20170101, which takes into account nodal effects. The Mean High and Low Water Spring (MHWS, MLWS) tide is estimated to +/- 62.9 cm respectively.

The ocean model HYCOM does a good job in reproducing the tidal signal with almost identical phases, but slightly lower amplitudes (Figure 23b+c). The wind-driven component can be estimated by subtracting a HYCOM water level based tidal prediction from the HYCOM water levels. This is shown in the Figure 23d for all the 11 years (2010-2011) for July-September, and by the green line in the other figures. The surge part (the residual) has a maximum of about 40 cm, which is about half of the tidal spring amplitude. However this value might be slightly underestimated, as the wind effect within the fjord is poorly represented by the relative coarse atmospheric model ERA5, which was used as forcing to the HYCOM_CICE model for that time period. However, surges are generated on larger scales, and the surge effect from the open waters from the Greenland Sea is well described in ERA5, which is the major forcing of importance for surges.

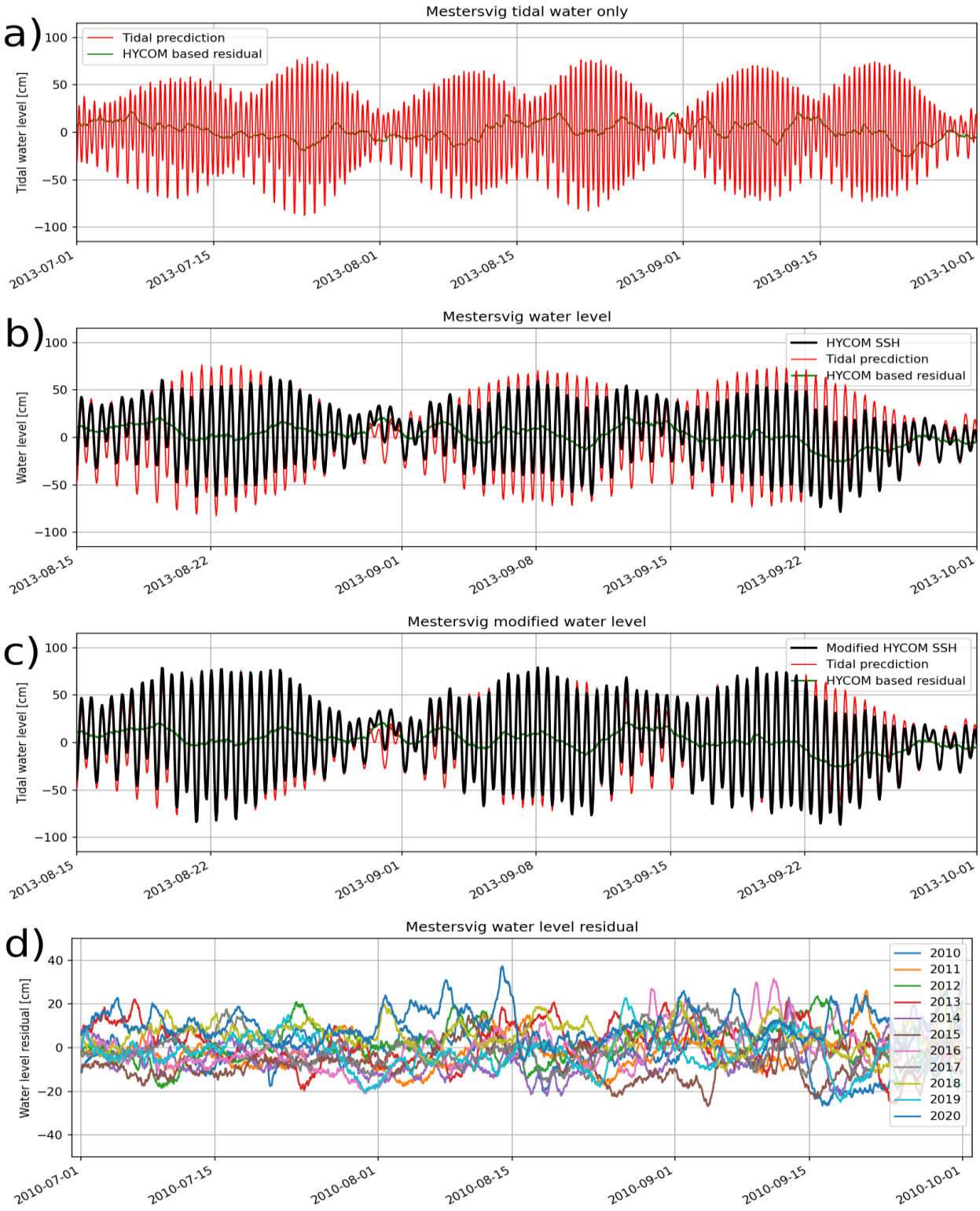

Figure 23: a) Tidal prediction (red) and HYCOM residual (green) for July-September 2013. b) HYCOM modelled sea surface height (SSH, black), tidal prediction (red) and HYCOM based residual (green). c) As above, but modified HYCOM SSH using existing tidal constituents but HYCOM residual. d) Modelled July-September residuals for 2010-2020 based on the HYCOM model.

In addition to the total water levels due to tides and surge effects, wind waves and swells also gives a contribution for the maximal water level. Furthermore, it is important to notice, that rolling icebergs may produce waves with amplitudes higher than the total contribution of tides and surges.

Tide tables for Mestersvig can be freely downloaded from www.dmi.dk and ocean.dmi.dk/tides/.

7 Conclusion

The present report provided a lot of statistics from Kong Oscar Fjord and its surroundings waters.

The fjord is characterized by less iceberg density compared to northerly fjords and Scoresbysund Fjord in south. In general, the Fjords becomes virtually free of sea ice during a continuous period ranging from two (mid-August to mid-October) to almost four (mid-July to mid-November) months. However, in exceptions, no parts of the fjord become completely free of sea ice during the summer. The outer parts of the fjord are in some years characterized by the presence of sea ice (mostly in lower concentrations) interrupting the open-water season. This is most pronounced at the outermost part of the fjords where “Storisen” sometimes may enter the outer part of the fjord.

The wind condition is much more calm within the fjord compared to outside. Outside the fjord the mean wind conditions ranging from 4-6 m/s in average, but frequency the area experience higher wind speeds. In 25% of the time, the wind speed exceeds 8 m/s, and 10 m/s five days in average every month. In average one day per month, but not necessary related to one single event, the off shore wind speed exceed 12-16 m/s or even more.

The visibility within the fjord is in general better compared to offshore. The visibility offshore is highly related to the sea ice condition. In general the visibility is low 25% of the time.

The ocean currents is in general southward within the East Greenland Current and in average in the order of 20 cm/s and similar for the sea ice drift. The ocean currents is also dominated by tides, which modifies the currents by about +/- 10 cm/s. Similar for the ice drift velocities, but these are also much affected by the winds.

The tide water at Mestersvig is semidiurnal with a large difference between nip and spring tide. The tidal range (low to high) is about 126 cm during spring tide corresponding to 63 cm in amplitude. Highest astronomical tide is 83 cm. The modelled wind generated surge part is below 40 cm.

8 References

CARRA, 2021. https://cds.climate.copernicus.eu/cdsapp#!/dataset/reanalysis-carra-single-levels

Haiden, T, Janousek, M, Vitart, F, Ben-Bouallegue, Z, Ferranti, L, Prates, F, 2021. Evaluation of ECMWF forecasts, including the 2021 upgrade. DOI: 10.21957/90pgicjk4

Hersbach, H., Bell, B., Berrisford, P., Biavati, G., Horányi, A., Muñoz Sabater, J., Nicolas, J., Peubey, C., Radu, R., Rozum, I., Schepers, D., Simmons, A., Soci, C., Dee, D., Thépaut, J-N. (2018): ERA5 hourly data on single levels from 1979 to present. Copernicus Climate Change Service (C3S) Climate Data Store (CDS), DOI:10.24381/cds.adbb2d47

Hill, C.; Deluca, C.; Balaji; Suarez, M.; Da Silva, A., 2004. "The architecture of the earth system modeling framework". *Computing in Science & Engineering*. **6 (1)**: 18–28.

Hunke, E., Allard, R., Blain, P., Blockley, E., Fletham, D., Fichefet, T., Garric, G., Grumbine, R., Lemieux, J.-F., Rasmussen, T., Ribergaard, M.H., Roberts, A., Schweiger, A., Tietsche, S., Tremblay, B., Vancoppenolle, M., Zhang, J., 2020. Should sea ice modeling tools designed for climate research be used for short-term forecasting? *Current Climate Change Reports*, **6**, 121-136, doi:10.1007/s40641-020-00162-y.

Hunke E., Allard R., Bailey D., Blain P., Craig A., Dupont F., DuVivier A., Grumbine R., Hebert D., Holland M., Jeffery N., Lemieux J., Osinski R., Rasmussen T.A.S., Ribergaard, M.H., Roberts A., Roy F., Turner M., and Worthen D., 2021. CICE-Consortium/CICE: CICE Version 6.3.0 *Zenodo*, doi:10.5281/zenodo.5423913.

Mankoff, K. D., Noël, B., Fettweis, X., Ahlstrøm, A. P., Colgan, W., Kondo, K., Langley, K., Sugiyama, S., van As, D., and Fausto, R. S., 2020. Greenland liquid water discharge from 1958 through 2019. *Earth Syst. Sci. Data*, **12**, 2811–2841, https://doi.org/10.5194/essd-12-2811-2020

Metzger, E.J., O.M. Smedstad, P.G. Thoppil, H.E. Hurlburt, J.A. Cummings, A.J. Wallcraft, L. Zamudio, D.S. Franklin, P.G. Posey, M.W. Phelps, P.J. Hogan, F.L. Bub, and C.J. DeHaan. 2014. US Navy operational global ocean and Arctic ice prediction systems. *Oceanography* 27(3):32–43, https://doi.org/10.5670/oceanog.2014.66.

9 Previous reports

Previous reports from the Danish Meteorological Institute can be found on:
https://www.dmi.dk/publikationer/